ESTIMATION OF TEMPERATURE RISE IN ELECTRICAL MACHINES

A DISSERTATION
Submitted in partial fulfilment of the
requirements for the award of the Degree
of
MASTER OF ENGINEERING
in
ELECTRICAL ENGINEERING
(Power Apparatus And Electric Drives)

By
DEEPA

DEPARTMENT OF ELECTRICAL ENGINEERING
UNIVERSITY OF ROORKEE
ROORKEE, 247672 (INDIA)
November, 1979

CERTIFICATE

CERTIFIED that the thesis entitled "[illegible] OF [illegible] IN ELECTRICAL MACHINES" which is being submitted by [illegible] in partial fulfilment of the requirements for the award of the DEGREE OF MASTER OF ENGINEERING IN ELECTRICAL ENGINEERING (Power Apparatus and Electric Drives) at the University of Roorkee is a record of student's own work carried out by her under the supervision and guidance of the undersigned. The matter embodied in this thesis has not been submitted for the award of any other degree or diploma.

This is further certified that she has worked for a period of 10 months from January 15, 1979 to November 11, 1979 for preparing this dissertation at this University.

ROORKEE

NOV. 15, 1979.

(Dr. [illegible])
Reader
Department of Elect. Engineering
University of Roorkee
Roorkee

(Dr. [illegible])
Professor
Department of Electrical Engineering
University of Roorkee
Roorkee

ACKNOWLEDGEMENT

I express my deep sense of gratitude to Dr. N.D.Sharma, Professor, Electrical Engineering Department, University of Roorkee, Roorkee, for his guidance in this dissertation work.

I am grateful to Dr. S.C. Sharma, Reader, Electrical Engineering Department, University of Roorkee, Roorkee, for his constant encouragement, systematic guidance and keen interest throughout this. I am highly indebted to him for all the help and expert guidance he provided on problems that came up time to time.

I am also thankful to Dr. L.M. Ray, Professor and Head, Electrical Engineering Department, University of Roorkee, Roorkee, for providing necessary facilities.

Last but not the least, I am thankful to the Workshop Staff, Laboratory Technicians for their cooperation.

ROORKEE

NOVEMBER 15 ,1979.

Deepa

DEEPA

C O N T E N T S

ABSTRACT

Temperature of Electrical Machines rises because of over loading, repeated starts, locked rotors and faulty conditions. Hence overheating of machines takes place, which reduces the life of machine. The previous knowledge of the temperature rises in different parts of machine is necessary to solve these problems.

In this dissertation estimation oftemperature rise in electrical machine is described using theoretical and experimental approaches.

Thermal equivalent circuit approach is used for theoretical estimation of temperature rise. A new instrumentation scheme has been developed for the estimation of temperatures at hot-spots in both stator and rotor of an electrical machine. Sensors Thermistors have been used as temperature sensors.

This estimation of temperature rise in electrical machine is useful to improve the design. This is also useful for providing protection to electrical machine.

CHAPTER 1

INTRODUCTION

Present day designers tend to utilize the maximum capability of motors i.e. largest possible output from a motor for a given cost. Machines may be severely damaged by overheating due to over loading, repeated starts, locked rotors, mechanical stalling and in many instances unbalanced phase currents.

Overheating of insulation greatly accelerates the aging process causing the chemical-mechanical degradation which results in electric break down.

Implicit in most operating procedures is that the temperature is known for the hottest parts for the loading conditions.

In the case of thermal circuits of motor 'heating above limits' should not be misunderstood. A motor does not have one temperature but has a temperature spectrum. Rotor-slot conductors have one temperature, and rings another, stator iron a third, rotor bars a fourth and so on through many differentials. These temperature differences produce continual transfer of heat between elements at a rate determined by the magnitude of the differences and the thermal impedances. 'Heating above limit' means there will be thermal or mechanical strain (strain resulting from heat such as expanding and contracting fabricated joints on the rotor) great enough to affect normal motor life as defined by the designer.

Now-a-days the trend in motor design is reduction in size and lowering of cost which is generally achieved by more efficient use of improved materials. Motor manufacturers are utilising higher temperature insulating materials in new and better designs. Other improvement such as higher grade steel and better ventilation techniques are contributing in the reduction of motor size and cost. Even though these new techniques are providing increased margin of operation at higher design temperatures, motor will still overheat if not properly limited under all conditions of abnormal operations. Because of the compact design of new motors, their rates of temperature rise for abnormal conditions are considerably higher. Thus it is of increasing importance to estimate the temperature rise of different parts of machine more precisely.

From protection point of view some knowledge of the motors design characteristics must be available together with specific class of insulation with the manufacturer. Design characteristic includes temperature rise which can be calculated for steady state as well as the transient conditions.

From a motor application point of view long life of winding insulation and operation at higher than rated temperature are incompatible. When overheating takes place the useful life of winding is reduced. This also reduces the life of insulation to half for each 8 to 10°C increase in continuous temperature above a certain limit. But it is unaffected by transient moderate over temperatures.

The temperature corresponding to overload (i.e. ± 10% rated voltage or ± 5% rated frequency on combined) conditions represent the required level for expected or planned motor operation.

The advent of conductor cooling has allowed current densities to approximately 9 and this increases the rate of heat generation to approximately four times that of previous levels[1]. There is a great need for direct measurements of local rotor temperature because of the following reasons :-

(a) The relative effectiveness of the thermal conduction through the copper in limiting the 'hot-spot' rise in local regions will be reduced approximately a 25% of its former level.

(b) The ratio of the rate of I^2R heat generation in the winding to the thermal storage capacity is much higher so that transients tend to proceed more rapidly.

(c) In all conductor-cooled rotors a substantial part of the total copper rise at any point is 'surface rise' between the conductor and the cooling gas. Surface rise varies inversely with the local heat transfer coefficient which is often difficult to predict precisely. This is particularly true in regions where the flow path geometry changes abruptly or where the coolant flow is allowed to divide among several parallel paths which are fed from or discharge to a common manifold chamber or array. The proper evaluation of the local heat transfer coefficients is further complicated by 'free convection' effects.

(d) Conductor cooled rotor have been built in many ways resulting in widely different ratios of hot-spot to average temperature rise. Consequently different designs can not be compared on the basis of average temperature rise and the standards which are written for conventionally cooled machines and specify only the average rotor temperature rise, should not be applied directly.

(e) In all the designs a great number of flow circuits differ in major or minor detail to accomodate differences between the inner and outer coils, the end windings and body portions of the winding and so forth. Local measurements are necessary to ensure that the flow circuits are performing as designed. When only the average temperature for the entire winding is measured a local problem might go undetected.

Broadly speaking, there are two approaches for the estimation of temperature rise in electrical machine. One is theoretical estimation of temperature rise in a machine. Theoretical estimation is done at the design stage and then prototype model is made. Experimental measurements of temperature are made for this prototype model to see whether machine is performing as designed. There are always errors in both measured and calculated values. Hence this becomes an iterative method to improve design. We are interested to search a solution which gives satisfactory agreement between measured and calculated temperature with less number of iterative processes. Hence this whole design process becomes

economical. The whole problem is also important for protection view point. If we know the temperature distribution at designed stage then we can put sensors at hot spot to measure temperature. We can also put relay for protection view point.

In this dissertation the main aim is to develop a method for the estimation of temperature rise of different parts in electrical machine. Chapter I gives the introduction and importance of the problem of heat-transfer. Chapter II deals with the review of different methods used for estimation of temperature rise. In chapter III theoretical method based on development of thermal equivalent circuit[13] for estimation of temperature rise in electrical machine has been discussed. As an example detailed calculations are done for a 3 phase slip ring induction motor. The temperature rise calculation have also been carried out for the test motor for verification of experimental results. Chapter IV deals with a new instrumentation scheme which has been developed for the measurement of hot spots temperatures in both rotor and stator. General discussion and conclusion are given in the last chapter.

CHAPTER II

REVIEW OF VARIOUS METHODS USED FOR DETERMINATION OF TEMPERATURE FIELD

This chapter deals with the review of various methods used so far by different designers and investigators for the estimation of temperature distribution in electrical machines. These methods may broadly classified into two categories.

1. Theoretical methods 2. Experimental methods.

2.1 THEORETICAL METHODS

Theoretical methods are generally used to predict the temperature rise of different parts of machine at the design stage to accomplish this a very careful study of all possible modes of heat transfer (conduction, convection, radiation) are considered.

The best method known for evaluating temperature distribution and all significant heat flow paths within a motor is a thermal circuit analogue approach. The thermal circuit is constructed by dividing the motor into a number of sections. The motor losses within each sections are lumped, and are generally inserted at the mean temperature of each section. To connect together the various sections of the motor, the mean temperature of each sections are connected with the appropriate thermal resistances. For determining, the proper thermal resistances, the partial differential equation of heat conduction may be solved.

$$\lambda x \frac{\partial^2 \theta}{\partial x^2} + \lambda y \frac{\partial^2 \theta}{\partial y^2} + \lambda z \frac{\partial^2 \theta}{\partial z^2} + p = 0$$

This is a three dimensional equation of heat flow. λx, λy and λz are thermal conductivities along x,y, and z directions in the elementary volume of the body under consideration.

p = Quantity of heat or specific losses in the unit volume in watts/cm^3

Various approaches viz. Graphical, Analytical, Numerical, analog have been used to solve the above mentioned heat conduction equation. Each approach has its own merits and demerits.

Taterberg[2] has developed a solution of the steady state flow of heat in large turbine generators by using analytical approach. A part of stator or rotor core section is studied. To maintain the general nature of the problem the existence of the following losses has been considered 1. Copper losses- These are generated in the slot insulation and flow through the insulation layer into the tooth, whence they continue radially and axially to the cooling medium. 2. Iron losses - These are generated in the core material itself when they flow axially and radially to the cooling medium. 3. Surface losses - These are assumed to be generated at the airgap surface of the core and are dissipated directly to the cooling air.

He has considered that there is no appreciable flow of heat in the tangential direction. A considerable flow takes

the teeth, but since their dimensions are relativ
resulting temperature variations may be neglected.
or copper. The problem is thus reduced to two-
problem, the main direction of flow being radial
Basic heat flow laws have been followed to obtain
suit.

In constructing an equivalent thermal circuit for
an uncertainty with regard to its construction will
it will be very small practically. Because in the
radial component of the flow of heat in the teeth
very small so that the influence upon the teeth
the core is also small. Hence he has assumed that
losses are uniformly distributed throughout the
the rotor, no core losses exist and the radial
ZO.

The solution obtained by this technique is usually
ly accurate for practical problem, but the errors
ined are coming because of neglecting some of the
f the actual problem.
accuracy of the approximate solution of the two-
mal problem with distributed losses. The initi
al circuit gives too high a value of mean temperat
ne the interference of the radial and axial flow h
neglected. The error is greatest when the flow is
o same intensity in the two directions. The error
an temperature of 6% is present from the source.
conclusion applies to the cases in which slot insu
[illegible] so that the copper losses enter the teet

at uniform density. But for low voltage machines and for rotor, where this is not the case, there is an additional error. This may account to 7% of error in the mean temperature.

(2) The taper of the teeth also leads to inaccuracy in the result. Then as in the rotor, there are no iron losses, the n taper will modify the flow of heat in the teeth. When there are iron losses, as in the stator, the tapered teeth will have much higher flux density at the tip than at the root. The resulting concentration of the iron losses at the tip will be very much pronounced and this will in turn modify the radial (and to a less extent the axial) flow of heat.

(3) The influence upon the temperature of irregular distribution of the losses is intimately connected with the specific thermal resistances of the copper and the teeth material. Copper losses consists of two parts (1) due to d.c. resistance (2) due to eddy current losses. The specific thermal resistance of iron in the teeth does not vary a great deal from machine to machine.

Johnson[3] has done analysis of heat flow within an enclosed motor. He has done this analysis under steady state as well as transient state. He has also used basic heat-transfer laws and thus obtained thermal resistance —

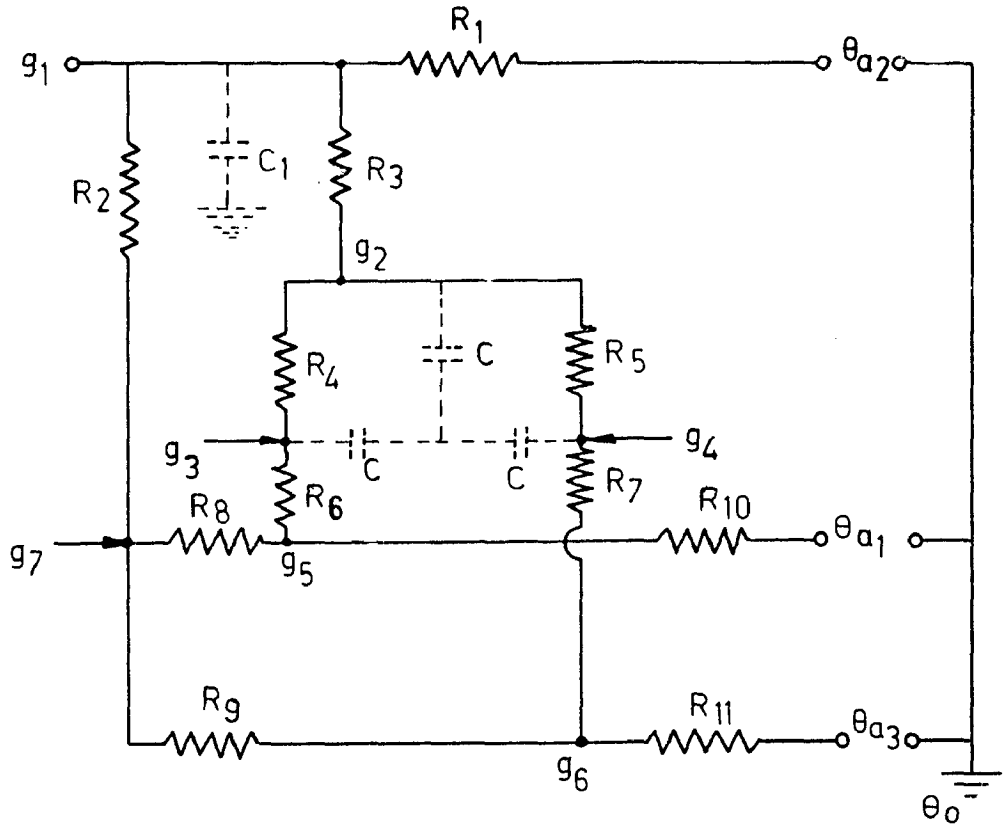

FIG. 1 _ THERMAL CIRCUIT FOR TOTALLY ENCLOSED I.M. WITH A CAST ALUMINIUM SQUIRREL CAGE MOTOR

$$R = \frac{1}{hA} + \frac{L}{kA}$$

where h = heat [illegible] efficient watts/inch^2.C

A = Area [illegible] flow (inch^2)

L = Effective length of conduction path inch

k = Thermal conductivity watts/inch.C

We represented storage of heat energy by a capacitor where capacitor $C = C_p.E.V$

C_p = Specific heat $\left(\frac{\text{watt-sec}}{\text{Pound-C}}\right)$

E = Density $\left(\frac{\text{Pounds}}{\text{inch}^3}\right)$

V = Volume (inch^3)

For determining proper thermal resistances the partial differential equation of heat conduction is shown

$$\rho C \frac{\partial \theta}{\partial t} = kx \frac{\partial^2 \theta}{\partial x^2} + ky \frac{\partial^2 \theta}{\partial y^2} + kz \frac{\partial^2 \theta}{\partial z^2} + q$$

The thermal circuit thus obtained is shown in Fig.1.
We has solved this 3-dimensional heat conduction equation by analytical approach. But this requires long and laborious hand calculations. So use of accurate and high speed computer makes this scheme very attractive. Computers are generally classified as either analog or digital.

The d.c. network analyzer and the electronic differential analyzer are two analog-type computers well suited for thermal circuit analysis. Differential analyzer is used to solve

transient-type problems. But the disadvantage of this is the need to compute the coefficients of differential equation. Scaling the problem to fit the computer is a problem in any analog solution, but is more difficult on differential analyzer than on d.c. network analyzer. For steady state solution the d.c. analyzer need only consist of variable resistors, adjustable current inputs and associated circuit to allow measurement of resistances, currents and voltages in the network. Transient problems are solved on the d.c. analyzer by incorporating variable capacitors, constant current sources, and multichannel recording equipment for recording the circuit temperature as a function time. If a thermal circuit is used frequently, or iteration is required for, sufficient accuracy, a digital computer will prove more convenient. Digital computer is recommended for short problems that and solved in frequently. The size of the circuit is limited only by the number of resistors available, since the losses may be inserted one at a time if necessary, and total temperature may be obtained by summing the results for each loss. The digital computer allows a detailed step-by-step analysis of rotor temperature that has not previously been practical.

Roseberry[4] has done analysis of transient stalled temperature rise of cast-aluminum squirrel cage rotor for induction motor. Empirical formula is being used to calculate capacitance.

$$C = C_p \cdot \theta \cdot V, \text{ and, Resistance, } R = \frac{1}{hA} + \frac{L}{kA}$$

both formula are similar as discussed by Johnson[3]. He has set the heat conduction equation in the form which is convenient for use on an Analog computer. Thus temperature rise is obtained.

The motor used by him was 4 Pole, 50 H.P. polyphase induction motor. All calculations and tests were made for the case of full voltage stall with balanced voltages applied. A close agreement between calculated and test results was obtained both in magnitude and the shape of the time-temperature curve.

He has also suggested an alternative method of solution of equivalent thermal circuit by setting up an analogous electrical circuit with resistors and capacitors, apply the current input and read desired voltages in the circuit with a recorder. Application of appropriate scale factors makes it possible to use practical circuit components.

Vesely[5] has also carried out the determination of the transient temperature distribution in a turbo-alternator rotor. He has solved this problem for unidirectional flow, although the method holds for three-dimensional flow. He has solved heat-conduction equation by means of an analog technique. Values of the heat transfer coefficient resulting from a given gas velocity in channels and ducts may be computed from the empirical formula given by Mc Adams[6].

The results obtained by Vesely[5] are -
(1) Temperature rise/time curve for copper is not of double exponential form (2) The surface loss causes a reduction in

temperature gradient across the slot top insulation and takes negligible difference elsewhere, the heat from the surface loss concentrating mainly in the rotor steel (3) Heating and cooling temperature /time curves are not mirror images. (4) Temperature rises are low compared with those obtained with copper loss o owing to the large proportions of heat flowing directly into the stator-rotor gap. (5) Temperature in the iron are more affected by the surface heating than those in the copper. This is because the heat flow in much greater quantity through the low-thermal iron than through the high resistance of the slot insulation.

Two papers of heat flow in the stator core of large turbine generators, by the method of three dimensional finite elements has been discussed by Arnor and Chari[7,3]. In part I of this paper author has given a general derivation of the variational formulation for three-dimensional scalar potential field problem.

In part II of the paper, the heat conduction equation and its variation formulation has been described briefly. The application of the finite element technique and 3-dimensional elements in particular to the stator core heating problem has been fully described.

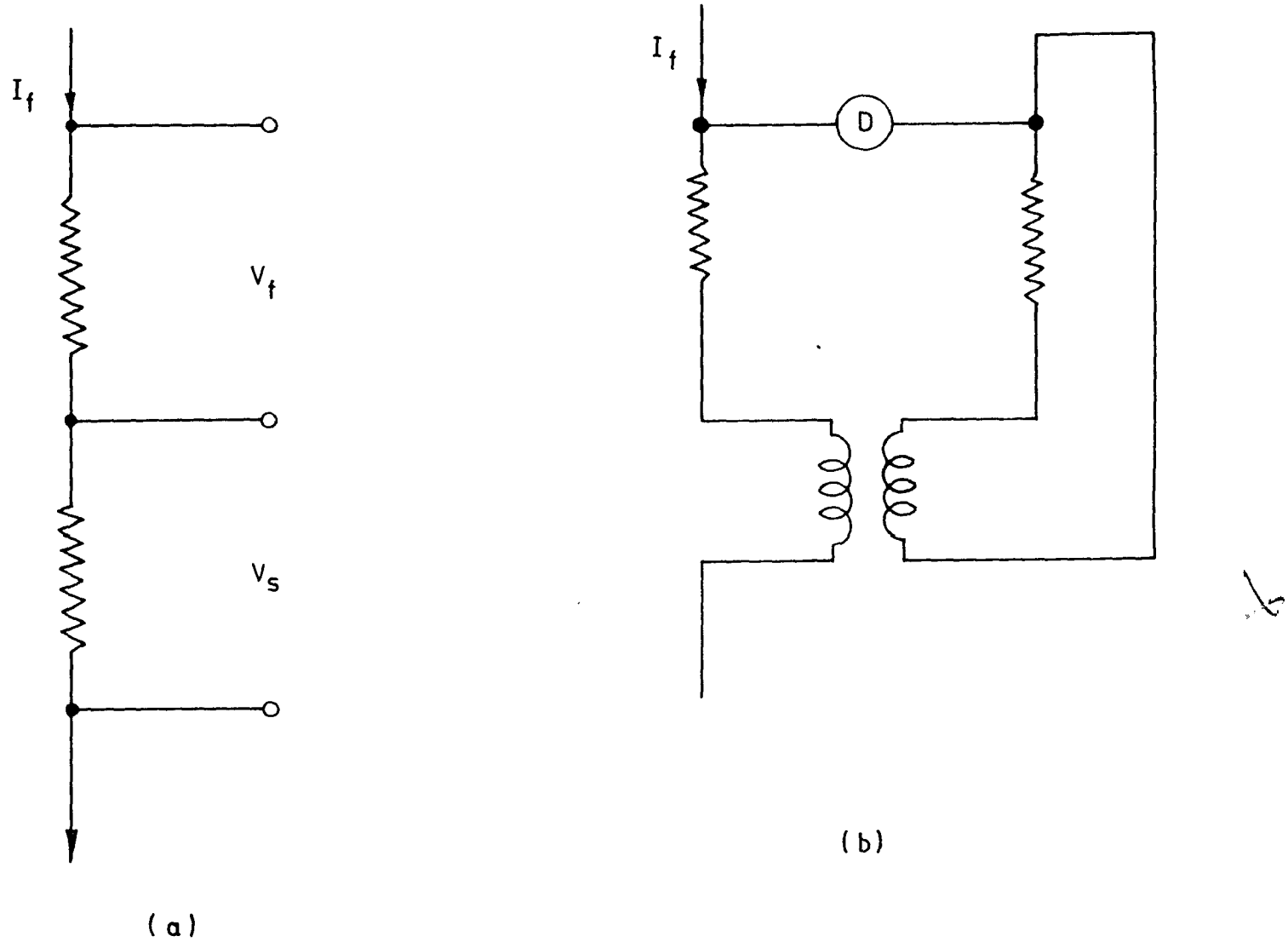

FIG. 2 _METHODS OF MEASUREMENT OF THE RESISTANCE OF THE FIELD WINDING

2.2 EXPERIMENTAL METHOD

Several experimental methods have been used for the measurement of temperature as far [9,10,11,12]. De Martin, et.al. (9) developed a technique for the measurement of temperature rise in a rotor of a large generator. A direct current comparator was used as basic block, which enabled accurate measurements from few percent to above 100 % of rated field current. The measurements were taken under various loading and cooling conditions. In this method average rotor temperature was measured by measuring the resistance of field winding by means of a self balancing d.c. comparator.

The resistance of the winding can be measured by passing the field current through a shunt and comparing the voltage across the winding and the shunt as shown in Fig.2(a). But this is not an accurate method. So in this method, it was improved by using a d.c. current transformer. The connection for the improved method are shown in Fig.2(b).

A d.c. current comparator was made with two toroidal cores of high permeability square-loop magnetic material, the pair of cores were totally enclosed in a hollow toroidal magnetic shield, over which were placed the ratio winding that generates a signal at twice the oscillator frequency, which was used to control an amplifier which in turn drove a current through the other ratio winding to make the net flux in the approach zero. Thus the self balancing d.c. comparator acted like an accurate current transformer which could operate at zero frequency.

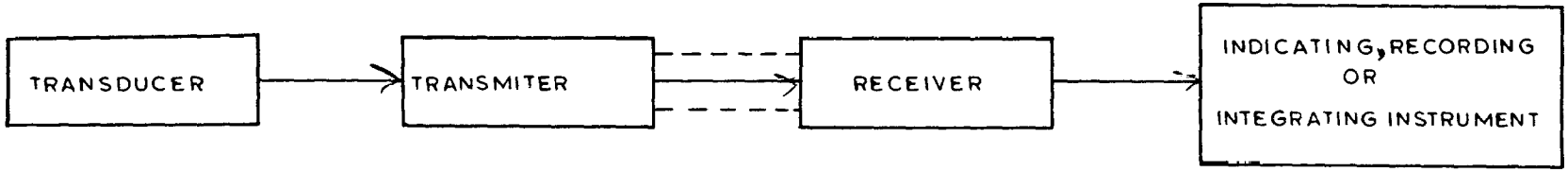

FIG. 3 _BASIC TELEMENTRY SYSTEM

The accuracy of the measurement of resistance change of field winding was within 0.1 % to calculate the temperature rise within 0.25°C for the coefficient of resistance of the copper winding as 0.425 %/°C. The errors of the comparator were very small ofthe order of IPPM (Part per Million).

While the generator was turning slowly on the turning gear, the apparent impedance of the rotor varied with position. This variation which repeated once each revolution, was attributed to residual magnetism in the stator iron, which generates a voltage in the field windings which was a function of the rotor position and hence the error in measurement was observed.

The above method has some limitations and can not be used for the measurement of temperature in case of large rating brushless turbo generators. Telemetry techniques are used for such cases. A general description of telemetry technique is given below[15].

Telemetry Technique

According to the American Standard Association Telemetry is the indicating, recording or integrating of a quantity at a distance by electrical translating means.

Any telemetry system can be divided into four components A block diagram of the basic telemetry system is shown in Fig.3.

Transducer

It is a sensing device for converting the measured quantity into a proportional electrical signal.

The following features should be emphasized upon while making selection of telemetry system :-

1. Fast response
2. High accuracy
3. High reliability
4. Good stability
5. Convenience and stability of calibration
6. Easy maintenance
7. Minimum limitations on channels.

Importance of Analog-Telemetry Technique

(1) Continuously changing operational events can be indicated more clearly by this method and can also be used as analog recorded diagrams.

(2) It is very convenient to compare several measurements with one another or with their available nominal values eg of several diagrams eg. daily records with one another.

(3) Clarity is absolutely necessary for the rapid survey of different operational processes and can not be attained with digital indicating equipment.

(4) It is easier to detect the tendency of changes in the measurand on an analog recording.

(5) To recover the data it is very essential that the transmitter and receiver equipments operate in synchronism. Each bit transmitted must be synchronised in time and phase with the bit generated at the receiving end. Data can only be recovered if there is bit, word and frame synchronization.

The accuracy of the measurement of resistance change of field winding was within 0.1 % to calculate the temperature rise within 0.25°C for the coefficient of resistance of the copper winding as 0.425 %/°C. The errors of the comparator were very small of the order of PPM (Part per Million).

While the generator was turning slowly on the turning gear, the apparent impedance of the rotor varied with position. This variation which repeated once each revolution, was attributed to residual magnetism in the stator iron, which generates a voltage in the field windings which was a function of the rotor position and hence the error in measurement was observed.

The above method has some limitations and can not be used for the measurement of temperature in case of large rating brushless turbo generators. Telemetry techniques are used for such cases. A general description of telemetry technique is given below[95].

Telemetry Technique

According to the American Standard Association Telemetry is the indicating, recording or integrating of a quantity at a distance by electrical translating means.

Any telemetry system can be divided into four components. A block diagram of the basic telemetry system is shown in Fig.3.

Transducer

It is a sensing device for converting the measured quantity into a proportional electrical signal.

Transducer

It is a device which is used for transforming and transmitting the output of transducer. The instrument combining the transducer and the transmission is known as sending end transducer.

Transmission Channel

This is the link between transmitter and the receiver. It can be of two types:-

(a) Physical link - like cables, aerial lines etc.

(b) Radio link - short or ultra short waves.

Receiver

It is a device which is used for retranslating the received signal into reading comprehensive reading, any deflection of an instrument pointer.

The aim of telemetry is to transmit continuously the measurement of a variable and to express that measured in readable form. During the transmission, a distortion of the auxiliary parameters may occur, in which case the receiver will respond to the modified value. Thus care should be taken to reduce these errors. This is done by proper selection of the transmission parameter. When the distance of transmission is large, e.g. and pulse telemetry systems are more suitable than the proximity telemetry system because in the pulse system the measurand is represented by the frequency, number, duration or phase of the pulses ; thereby, being independent of variations in line parameter.

The following features should be emphasised upon while making selection of telemetry systems :-

1. Fast response
2. High accuracy
3. High reliability
4. Good stability
5. Convenience and stability of calibration
6. Easy maintenance
7. Minimum limitations on channels.

Importance of Analog-Telemetry Technique

(1) Continuously changing operational events can be indicated more clearly by this method and can also be used as analog recorded diagrams.

(2) It is very convenient to compare several measurements with one another or with their available normal values as of several diagrams eg. daily records with one another.

(3) Clarity is absolutely necessary for the rapid survey of different operational processes and can not be attained with digital indicating equipment.

(4) It is easier to detect the tendency of changes in the measured on an analog recording.

(5) To recover the data it is very essential that the transmitter and receiver equipments operate in synchronism. Each bit transmitted must be synchronised in time and phase with the bit generated at the receiving end. Data can only be recovered if there is bit, word and frame synchronisation.

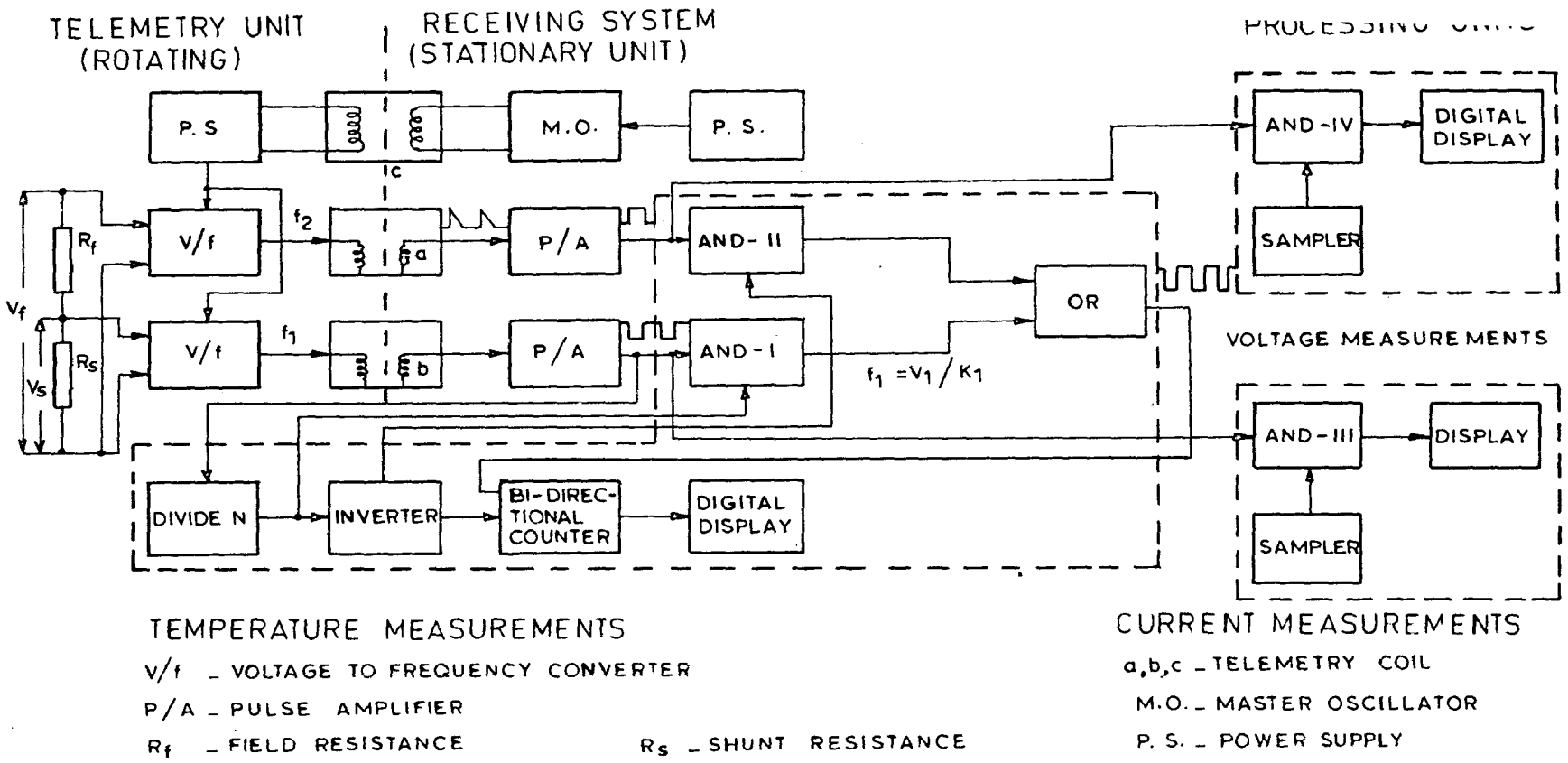

FIG. 4 - BLOCK DIAGRAM

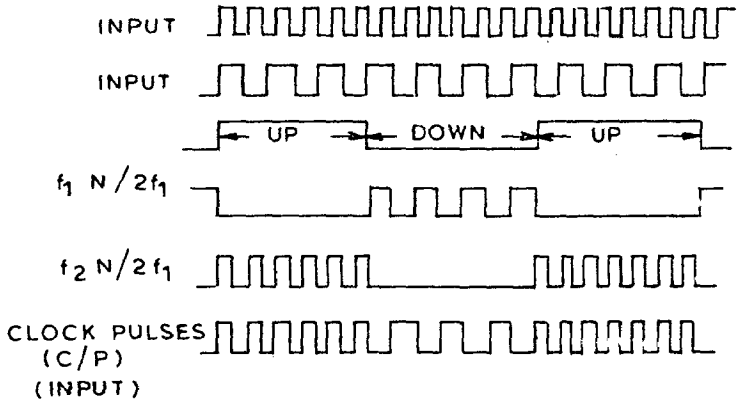

FIG. 5 - TIMING DIAGRAM

(6) The digital telemetry system is complex as compared to analog systems if the number of input channels is less.

(7) If it is compared component by component then digital equipment is more expensive than analog instrument.

Necessity of Analog Telemetry Over Digital Telemetry

Digital telemetry has higher communication efficiency, noise immunity, reliability, capability of handling both analog and digital inputs and offers system flexibility.

Gupta, et. al.[10] developed a temperature measuring method using telemetry technique. In this technique average temperature of field winding of brush brushless excitation system can measured. The voltage and current of field winding were measured. The rotor temperature can determined from the precise measurement of change of resistance of the field winding due to temperature rise.

The basic principle of this method for the measurement of temperature, voltage and current is explained with the help of Fig.(4) and Fig.(5). Field winding current is converted into a proportional d.c. voltage V_0, using a shunt resistor This voltage V_0 converted to frequency f_1. Display of this frequency after telemetry gives field winding current. Similarly field winding voltage V_f is also converted into frequency f_2. Display of this frequency after telemetry gives field winding voltage. This voltage divided by current is a measure of field winding resistance. This resistance is proportional to temperature. A digital display of temperature is also made.

Gramp et.al. and Kudlacik et.al.[11,12] developed methods for the measurement of temperatures of hot spots. In the method given by Gramp et.al., the direct measurement of stator winding copper temperature in large electric machine was made possible with a miniature tunnel diode oscillator mounted directly on the current carrying conductor. A temperature sensitive capacitor resonant circuit caused the radiated signal frequency to change with the change in copper temperature. The signal radiated through the thickness of winding ground insulation reached to antenna, external to the ground insulation. Then this signal was compared with one from a calibrated external oscillator using a standard A M (amplitude modulated) radio circuit. Calibration curve were drawn for frequency Vs temperature.

But later on this method was found to be very much inaccurate. Various investigators observed difference of more than 20°C when RTD (Resistance temperature detector) temperature were compared with copper temperature thermocouple.

(b) Kudlacik et.al.[12] made local rotor winding temperature measurement for large turbine generators by using thermocouples as sensor. The signal from rotor was transferred through instrument slip rings during heat runs at loading up to full-load field current. The accuracy of this measurement was found to be approximately ± 1°C. In this method for the measurement of temperature the errors were largely due to temperature difference between the "rotating studs" and "stationary study" at the slip rings.

CHAPTER III

SIMULATION FOR ESTIMATION OF TEMPERATURE DISTRIBUTION IN SQUIRREL CAGE INDUCTION MACHINE

3.1 DERIVATION OF BASIC HEAT CONDUCTION EQUATION

In this chapter a simple method for the estimation of temperature rise in 3-phase induction motor by using thermal equivalent circuit approach is discussed.

For this basic heat transfer laws are considered. Heat transfer in the cooling medium takes place by conduction in different parts of machine and by convection/radiation from the surface of that part. Heat transfer from the boundary of the heated surface and cooling air is obtained from Newton's law according to which the heat dissipated is given by

$$Q = \alpha.(\theta_1 - \theta_2).S$$
$$= \alpha.S.\theta$$

where θ_2 = Temperature of cooling medium

θ_1 = Temperature of part under consideration

S = Surface area

α = Coefficient of heat transfer of the surface

θ = Temperature rise.

$$\theta = \frac{Q}{\alpha.S} = \frac{q}{\alpha}$$

where $\frac{Q}{S}$ = q = Heat flux/unit surface area.

With the transfer of heat from the surface to the cooling medium, temperature gradient occurs in the coil insulation, in the stator and rotor core in the direction of heat flow Q. According to

fundamental law of heat conduction heat flux density in the direction of its flow is proportional to the temperature gradient in the opposite direction i.e. $q = -$ (cond θ, coefficient is called thermal conductivity, -ve sign is placed because in the +ve direction of heat flow, the temperature gradient is -ve i.e. in this direction temperature decreases.

In single dimension heat flow (for example in the direction of x - axis), we have grad $\theta = \frac{d\theta}{dx}$. The values of are given in Appendix-I. These values are obtained experimentally by different investigators. The value of depends upon the characteristic of the material. For electrical machine with heterogenous nature of each part, the poisson equation for heat conduction with internal source of heat is to be solved in 3-dimensions-

$$x \frac{\partial^2\theta}{\partial x^2} + y \frac{\partial^2\theta}{\partial y^2} + z \frac{\partial^2\theta}{\partial z^2} + p = 0$$

where x, y and z are thermal conductivities along x, y and z in the elementary volume of the body under consideration.

p = Quantity of heat or specific losses in the same volume in watts/cm^2

In the absence of heat sources in the volume under consideration and for a single dimension heat flow we have $x \frac{\partial^2\theta}{\partial x^2} = 0$.

i.e. $\theta = C_1 x + C_2$ where $C_1 = \frac{d\theta}{dx}$ = constant.

In this case temperature rises linearly with constant heat source, we will have -

$$\theta = \frac{p}{2\lambda} x^2 + C_1 x + C_2$$

C_1 and C_2 are obtained from boundary conditions

$$\theta_{mean} = \theta_{overhang} + \frac{pl^2}{12\lambda} \qquad \ldots (1)$$

$$\theta_{max} = \theta_{overhang} + \frac{pl^2}{8\lambda} \qquad \ldots (2)$$

9.2 DEVELOPMENT OF THERMAL EQUIVALENT CIRCUIT

Method of thermal equivalent circuit using the concept of thermal resistance and solving them on the method is applicable for electrical circuits is being widely applied for the design of electrical machines. For this parallel addition of thermal resistance is used for solving not only 2-dimensional but also 3-dimensional problems. Use of thermal equivalent circuits makes it possible to evaluate the mean temperature of the parts of electrical machines which are considered to be homogeneous body. Basic heat flow laws are used for calculating the temperature of each part of the machine

$$\theta_1 - \theta_2 = Q_{12} R_{12}$$

where θ_1 and θ_2 = Mean temperature of these points in $^\circ C$

R_{12} = Thermal resistance between two points 1 and 2 ($^\circ C/W$)

Q_{12} = Thermal flow between points 1 and 2.

It is natural that the larger the number of elements, the more accurate results will be obtained.

Machine can be divided into two parts, stator part and rotor part. Let the stator part be divided into 3-homogeneous bodies, consisting of sources of heat —

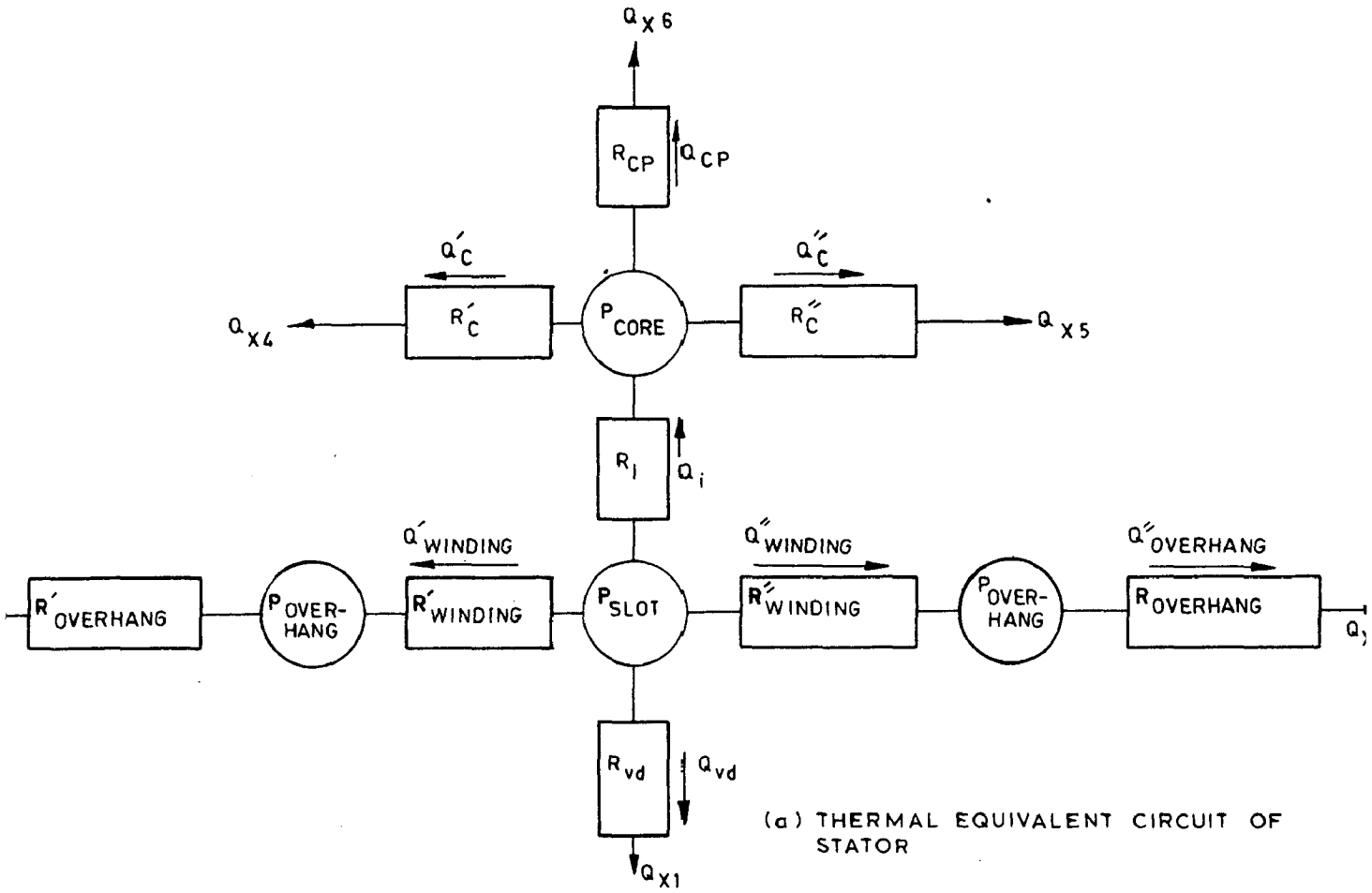

(a) THERMAL EQUIVALENT CIRCUIT OF STATOR

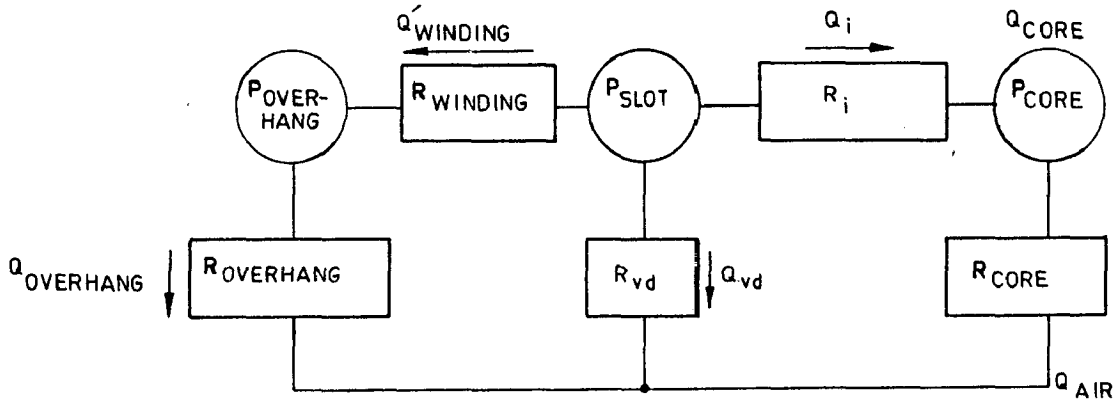

(b) SAME TEMPERATURE OF COOLING AIR AT ALL SURFACES

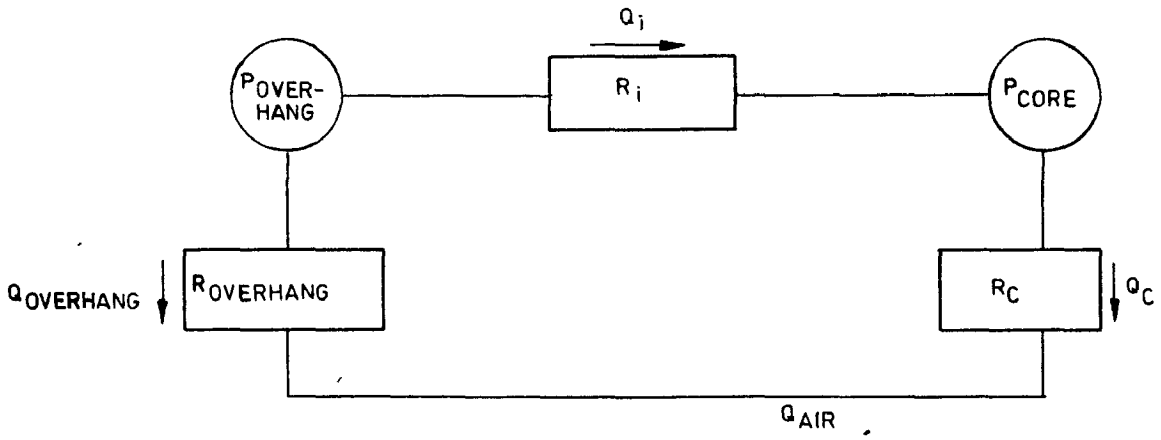

(c) SIMPLIFIED CIRCUIT WITH $R_{winding} = 0$

FIG. 6

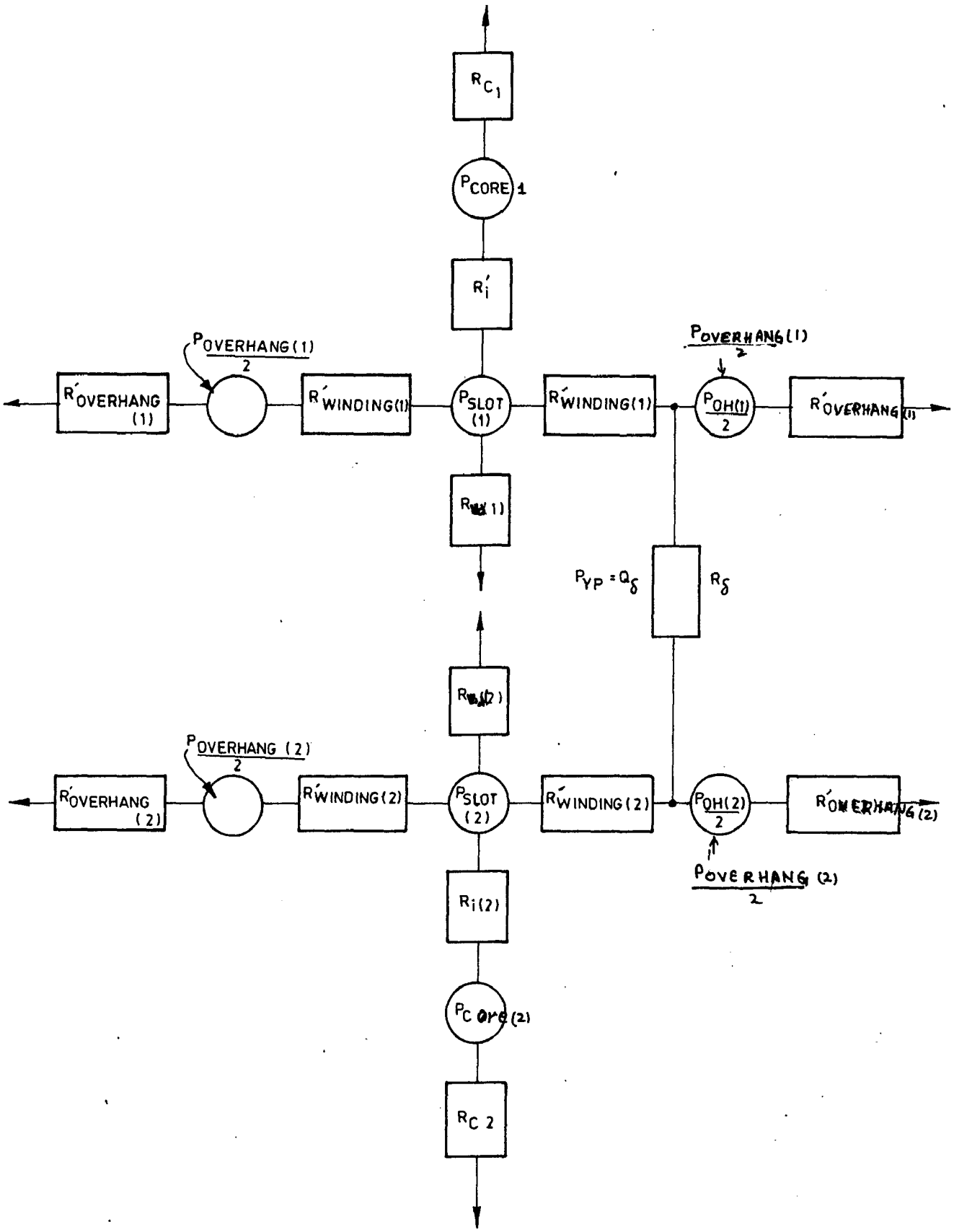

FIG.6(d)_COMPLETE THERMAL CIRCUIT FOR ELECTRICAL MACHINE

(1) Slot portion of the winding with losses P_{slot}

(2) Two sides of overhang portion with total loss $P_{overhang}$

(3) Stator core with losses P_{core}.

Each part gives heat flow. Considering general case that the conditions of the cooling of the parts under consideration are different. See Fig.6. Four paths of heat dissipation are considered.

Q_i = Heat flux to the tooth walls of the core with temperature drop in the thermal resistance of the slot insulation R_i

Q_{vd}= Heat flux to the cooling air in the radial ventilating ducts across thermal resistance R_{vd}.

$Q'_{winding}$ and $Q''_{winding}$= Heat flux from slot portion of the winding with temperature drop in the thermal resistance $R'_{winding}$ and $R''_{winding}$ along the conductor of the winding.

$Q'_{overhang}$ and $Q''_{overhang}$= Heat flux from overhang portion of the winding with a temperature drop in thermal resistance $R'_{overhang}$ and $R''_{overhang}$ to the air.

Q'_c and Q''_c = Heat flux from the surface of the core through sides of the packets with the temperature drop in the thermal resistance R'_c.

Q'_{cp} = Heat flux in the radial direction from the peripheral surface on the back of the stator core (air gap side).

To simplify the circuit assume that core temperature of

cooling air at all surfaces. Then $\theta_{s1} = \theta_{s2} = \theta_{s3} = \theta_{s4} = \theta_{s5} = \theta_{s6} = \theta_{Air}$. This is shown in Fig.6(b).

$R_{winding}$ and $R_{overhang}$ consists of parallel combination of the resistances $R'_{winding}$ and $R'_{overhang}$.

hence, $$R_{winding} = \frac{R'_{winding}}{2}$$

$$R_{overhang} = \frac{R'_{overhang}}{2} \qquad \ldots (3)$$

$$R_{core} = \frac{1}{\frac{R'_{core}}{2} + \frac{1}{R_{cp}}}$$

In Fig.6(b), there are 6 unknowns, θ_{slot}, $\theta_{overhang}$, θ_{core} are mean temperatures of slot portion of the winding, overhang portion and the core. Q_1, $Q_{winding}$, Q_{vd}, $Q_{overhang}$ and θ_{core} are the heat flows. For evaluating these unknowns following equations can be developed corresponding to Fig.6(b).

$$P_{slot} + P_{overhang} + P_{core} = Q_{overhang} + Q_{vd} + Q_{core}$$

$$Q_{overhang} = P_{overhang} + Q_{winding}$$

$$Q_{core} = Q_1 + P_{core}$$

$$\theta_{slot} - \theta_{air} = \theta_{vd} \times R_{vd}$$

$$\theta_{overhang} - \theta_{Air} = Q_{overhang} \times R_{overhang}$$

$$\theta_{core} - \theta_{Air} = Q_{core} \times R_{core}$$

$$\theta_{slot} - \theta_{overhang} = Q_{vd} \times R_{vd}$$

$$\theta_{slot} - \theta_{core} = Q_1 R_1$$

$$\theta_{Air} = \text{cooling medium temperature}$$

... (4)

As a result of solution of these simultaneous equations, we get the room temperature rise by putting $\theta_{Air} = 0$

$$\theta_{slot} = \frac{R_{winding} \times R_{cd} \times R_1 \left[P_{overhang}\left(1 + \frac{R_1}{R_{core}}\right) + P_{core}\left(1 + \frac{R_{winding}}{R_{overhang}}\right) + P_{slot}\left(1 + \frac{R_{winding}}{R_{overhang}}\right)\left(1 + \frac{R_1}{R_{core}}\right)\right]}{\left(R_{cd} \times R_1 + R_{cd} \times R_{winding} + R_{winding} \times R_1\right)\left(1 + \frac{R_{winding}}{R_{overhang}}\right)\left(1 + \frac{R_1}{R_{core}}\right) - R_{cd} \times R_1\left(1 + \frac{R_1}{R_{core}}\right) - R_{winding} \times R_{cd}\left(1 + \frac{R_{winding}}{R_{overhang}}\right)} \quad \ldots (5)$$

$$\theta_{overhang} = \frac{P_{overhang} \times R_{winding} + \theta_0}{1 + \frac{R_{winding}}{R_{overhang}}} \quad \ldots (6)$$

$$\theta_{core} = \frac{P_{core} \times R_1 + \theta_{slot}}{1 + \frac{R_1}{R_{core}}} \quad \ldots (7)$$

If we assume $R_{winding} = 0$, then the value of temperature decreases sufficiently. However, practically in the normal machine, this decrease is not much because of small value of $R_{winding}$. Thermal equivalent circuit with $R_{winding} = 0$ and its solution significantly significs. Simplified circuit is given in Fig.6(c). In this

$$P_{coil} = P_{slot} + P_{overhang} \quad \ldots (8)$$

$$R_{coil} = \frac{R_{winding} \times R_{w.d}}{R_{overhang} + R_{w.d}} \quad \ldots (9)$$

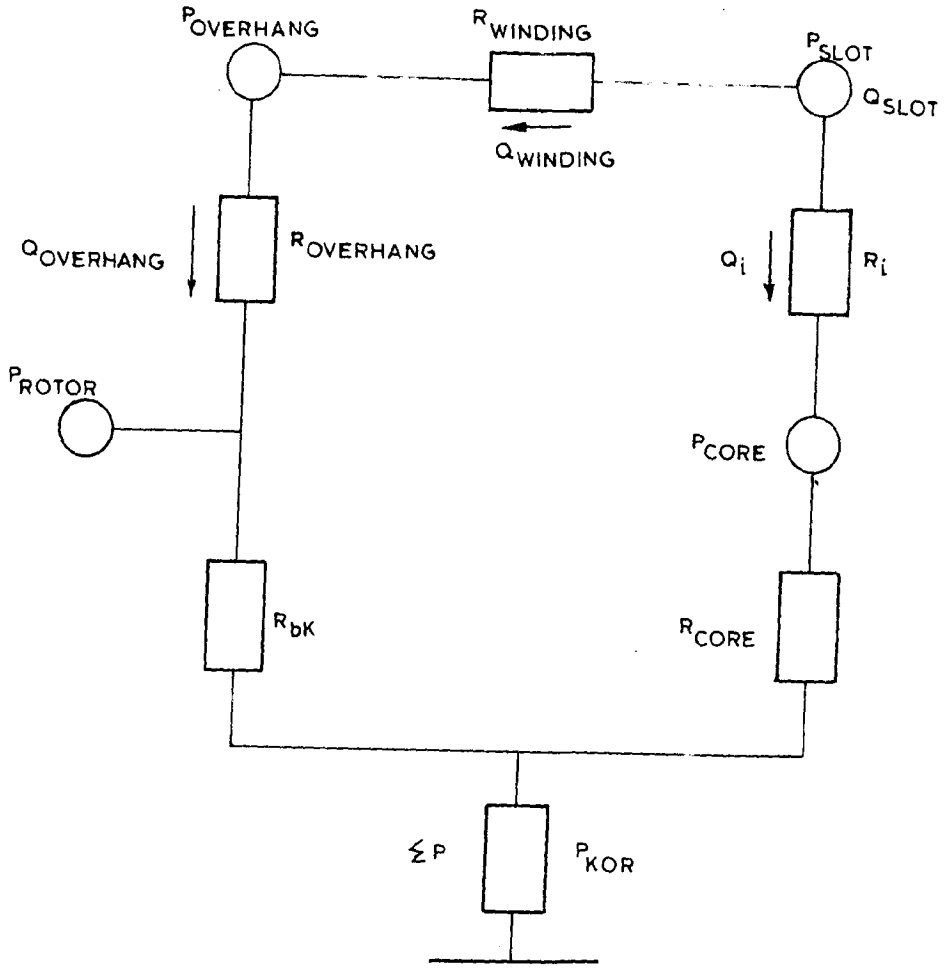

FIG. 7(a)_ THERMAL CIRCUIT FOR TOTALLY ENCLOSED MACHINE

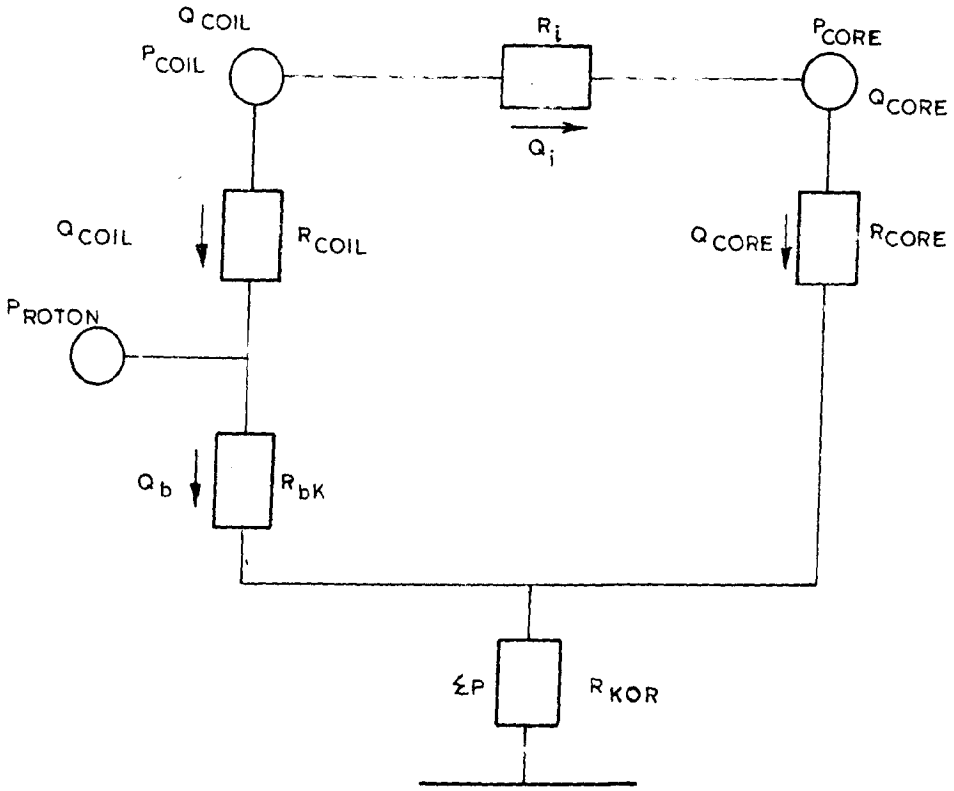

FIG. 7(b)_ SIMPLIFIED THERMAL CIRCUIT OF FAN COOLED MACHINE

$$\theta_{coil} = \frac{[P_{coil}(2a \frac{R_1}{R_{core}}) + P_{core}] R_{core}}{[1 + \frac{R_1}{R_{coil}} + \frac{R_{core}}{R_{coil}}]} \quad \ldots (10)$$

$$\theta_{core} = \frac{P_{core} \cdot R_{\delta} + \theta_{coil}}{1 + \frac{R_{\delta}}{R_{core}}} \quad \ldots (11)$$

Fig.6(c) gives thermal connection of stator and rotor which is depicted with the help of the thermal resistance of the air gap

$$R_{\delta}' = \frac{\delta}{Nu \cdot \alpha_{\delta}}$$

where, $\alpha_{\delta} = Nu \frac{\alpha}{2\delta}$

Nu = Nusselt's Number

α = Thermal conductivity of air

δ = Width of air gap in meters.

The thermal equivalent circuit is shown in Fig.7(a) is for totally enclosed, fan cooled machine. In the circuit, rotor losses are included, which include the copper losses and friction and windage losses. The thermal resistance R_1, $R_{winding}$, $R_{overhang}$, R_{core} are defined in the analogous manner in the preceding discussion.

Resistance R_{bH} characterises the temperature drop θ_b, θ_{HOU} between the heated internal air and housing. The resistance R_{HOU} is the temperature drop of the housing with respect to the room temperature of cooling air.

Thermal equivalent circuit of Fig.7-a is quite complex and consists of 10 unknowns defined by 10 different equations. Finding the formulae for calculation of the temperature rises of winding and core are cumbersome and inconvinient for calculations. In machines of small and medium power, upto 250 KW, temperature of the slot portion of the winding, θ_{coil} differs from the temperature of the overhang portion $\theta_{overhang}$ by a small amount. This fact is taken in Fig.7(a). By absence of $R_{winding}$, taking $R_{winding} = 0$, we get simplified equivalent circuit for the enclosed machine with 8 unknowns.

THERMAL METHOD FOR THE CALCULATION OF THERMAL RESISTANCES

3.3 CALCULATION OF THERMAL RESISTANCE FOR INSULATION

In calculations, mean value of thermal conductance of insulating material is considered, as the insulation consists of different materials. These values are obtained experimentally (See Appendix-1). The temperature drop is considered linear in insulation (heat source being absent).

Heat flowing Q across insulating layer of thickness δ is given by $\theta = \frac{\theta_1}{Q} - \delta$

θ_1 = Temperature drop (°C)

δ_1 = Thickness of insulation (cm)

σ = Thermal conductivity of insulation

a = cross sectional area (cm^2)

So $\theta_1 = \frac{Q\delta}{\sigma}$ (This is III to Ohm's law)

Thermal resistance (in $^{o}C/Watt$) $= \frac{\delta}{\lambda}$ ... (12)

For multilayer insulation the total temperature drop = Sum of the temperature drops in individual layers

$R_i = r_{i1} + R_{i2} + \ldots\ldots\ldots + R_{in}$

where $R_{in} = \frac{\delta_n}{\lambda_n}$

since $\delta_1 = \delta_2 = \delta_3 = \ldots\ldots = \delta_n$

so $\frac{\delta}{\lambda} = \frac{\delta_1}{\lambda_1} + \frac{\delta_2}{\lambda_2} + \frac{\delta_3}{\lambda_3} + \ldots\ldots\ldots$

so $= \frac{\delta}{\frac{\delta_1}{\lambda_1} + \frac{\delta_2}{\lambda_2} + \ldots\ldots \frac{\delta_n}{\lambda_n}}$

Thermal Resistance of Overhang Portion

$$R_{overhang} = \frac{\delta_i}{\lambda \cdot D_{overhang}} + \frac{1}{\alpha_{overhang} \cdot D_{overhang}}$$

where δ_i = Thickness of insulation of coil (cms)

$\alpha_{overhang}$ = Heat transfer coefficient of the peripheral surface of insulation (See Appendix II).

$D_{overhang}$ = Surface area of the overhang portion for single layer winding.

$D_{overhang}$ = Perimeter of coil x length of overhang x Number of stator slots

For two layer winding

$D_{overhang}$ = 2 x Number of stator slots x Perimeter of coil x length of overhang

1st part of this thermal resistance is coming from equation (12)

because of convection. 2nd part is owing because convection effect.

Thermal Resistance of Total of All Winding

From equation (1)

$$R_{winding} = \frac{l_1 + l_{overhang}}{2\delta \times \text{Number of slots} \times \text{Number of conductors in slot} \times \text{cross-sectional area of one conductor} \times \text{Thermal conductivity of metal}}$$

where l_1 = length of conductor

Thermal Resistance from Coil to the Cooling Air in Radial Ventilating Ducts

$$R_{vd} = \frac{\delta_i}{\lambda_i \times A_{v.d.}}$$

δ_i and λ_i are slot insulation thickness and thermal conductivities.

$A_{v.d.}$ = Area of heat conducting or transferring surface of the coil in radial ventilating ducts

= Number of stator slots × Perimeter of coil × width of radial ventilating ducts × Number of ventilating ducts.

Thermal Resistance R_a from (Stator/Rotor) Core to the Cooling Air

Heat transfer from the core takes place in the different directions depending upon system of ventilation. In forced ventilated machines with radial ventilating ducts heat is dissipated mainly from lateral surfaces on its path. It has one thermal resistance caused by the temperature drop between surface and cooling medium and other as a movement (flow) of heat along the cross section of the laminations to the lateral surfaces.

Thermal resistance R_{cq} in the perpendicular direction of the packets, to the cooling air is obtained from eqn. (2) as

$$R_{cq} = \frac{\lambda}{\alpha_q} + \frac{\ell'}{\sigma_q U_q}$$

α_q = Heat transfer coefficient in the radial ventilating ducts.

U_q = Lateral heat dissipating surface of all the packets

= $\pi (D_o - h_c) D_o (n_b + 1)$

D_o = Outside diameter of stator (cms)

h_c = Stator core height (cms)

ℓ' = length of the stator packet

σ_q = Thermal conductivity of core material + to the laminations (See Appendix I).

Heat is also dissipated from the cylindrical surface of the core. Heat transfer from the internal surface of the core with radial ventilating ducts is usually small because of the low speed of air near this surface.

Heat transfer from internal surface of the stator to rotor, across the air gap, may be sufficiently large with small value of the air gap.

With large air gap, heat transfer takes place corresponding to the indicated paths of heat flow shown in Fig.6(a) in the machine with radial ventilating ducts, to get -

$$R_{op} = \frac{\lambda}{\frac{1}{U_{ext}} + \frac{1}{U_{int}}} = \frac{1}{\alpha_{ext.} U_{ext} + \alpha_{int} U_{int.}}$$

$a_{ext.}$ = Heat transfer coefficient of the external surface of stator core packets = 0.0014 to 0.002 W/°C cm^2.

D_{ext} = External surface of the stator core packets

= $\pi D_o \ell' (n_D + 1)$

ℓ' = Actual length of one packet

a_{int} = Heat transfer coefficient of the internal surface of the core packet with large air gap from Fig. 8.

D_{int} = Internal surface of the stator packet.

Total thermal resistance with radial ventilating ducts is defined as $R_o = \frac{1}{\frac{1}{R_{eq}} + \frac{1}{R_{eD}}}$.

$R_{bK} = \frac{1}{a\ D_{bK}}$

a is taken from Appendix II.

D_{bK} = Internal surface of the carcase, covered by the air, includes (1) Internal surface of that part of carcase free from the stator core (2) Internal surface of end covers.

R_{KOR} is defined by the external heat dissipating surface of the carcase, large portion of which is the cylindrical surface of the carcase and a smaller portion is corresponding to end covers.

3.6 <u>SUMMARISATION AND CALCULATIONS FOR AN OPP 3-PHASE SLIP RING INDUCTION MOTOR</u>

As an example temperature rise calculations are presented

for 150 H.P. 3300 volts, 3 phase, 50 H.Z, 600 synchronous r.p.m. slip-ring induction motor in Appendix II. Full load efficiency for this motor = 0.91 and P.F. = 0.86. Whole design data for this machine is taken from the book by A.K. Sawhney (14).

3.5 TEMPERATURE RISE CALCULATIONS FOR EXPERIMENTAL MOTOR

Temperature rise calculations are also done for 5 H.P., 230/400 Volts, Δ/Y, 7.5 Amp., 3 phase, 1440 r.p.m. Induction motor in Appendix V. These calculations are made on experimental motor for comparison of experimental and theoritical results. No load test and Block rotor test is also performed for this motor to actually measure the losses in the motor (See Appendix IV).

Rating of 3-Phase Induction Motor

Δ-Y, 230/400 Volts, Δ/Y, 5 H.P., 1440 R.P.M., 7.5 Amp.

Stator dimensions

Number of slots = 36

Inside diameter = 14.75 cm

Outside diameter = 23.2 cm

Core depth = 2 cm

Core length = 10.8 cm

Slot depth = 2.2 cm

Slot width = 1.2 cm

Tooth width = 0.65 cm

Class A insulation = 15 mil. thick = 0.38 cm

winding number 25 S.W.G. (1.01 m.m. diameter) 0.2 cm insulation thickness.

length of yoke = 30 cm

Rotor dimensions

Number of slots = 36

Core depth = 3.6 cm

Core length = 10.8 cm

Slot depth = 1.6 cm

Slot width = 1.2 cm

Tooth width = 0.5 cm

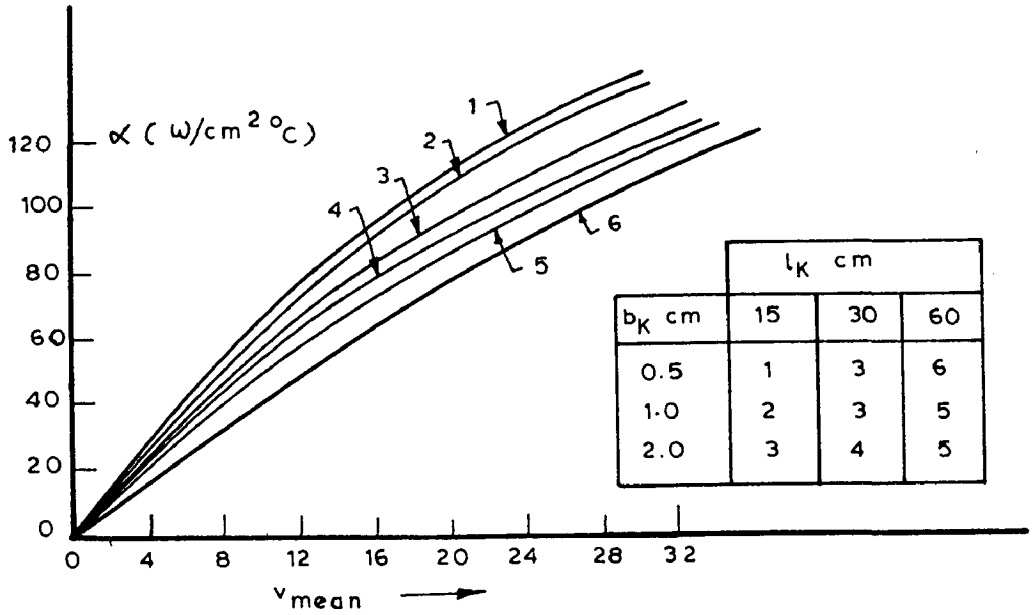

b_K cm	l_K cm 15	30	60
0.5	1	3	6
1.0	2	3	5
2.0	3	4	5

FIG. 8 (a) – HEAT TRANSFER COEFFICIENT α OF THE RADIAL VENTILATING DUCTS CURVES 1,2,3,4,5,6 CORRESPONDS TO DIFFERENT VALUES OF l_K AND b_K

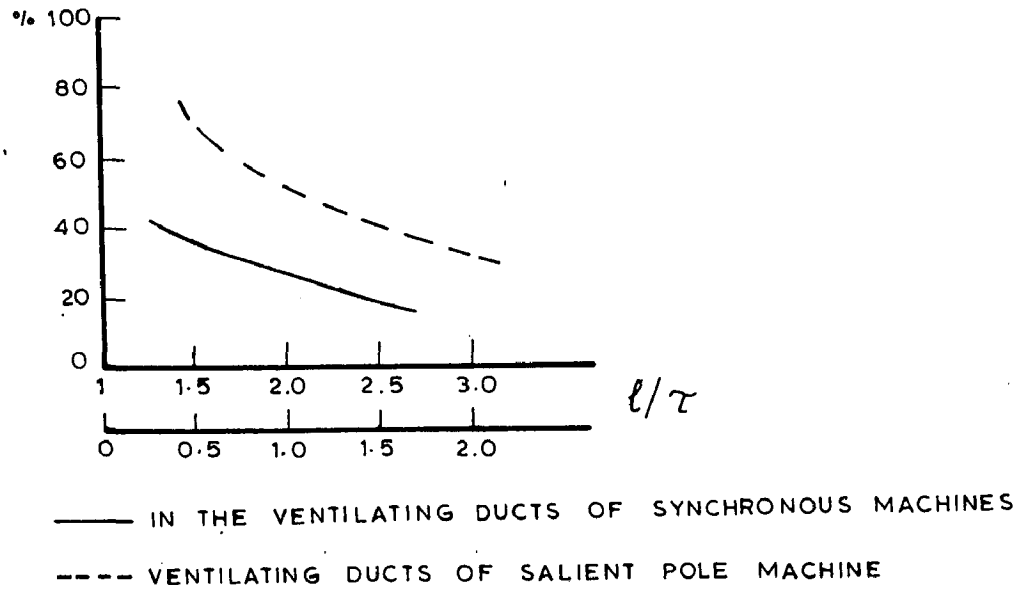

FIG. 8 (b) – MEAN VELOCITY OF AIR IN % OF ROTOR SURFACE SPECDS

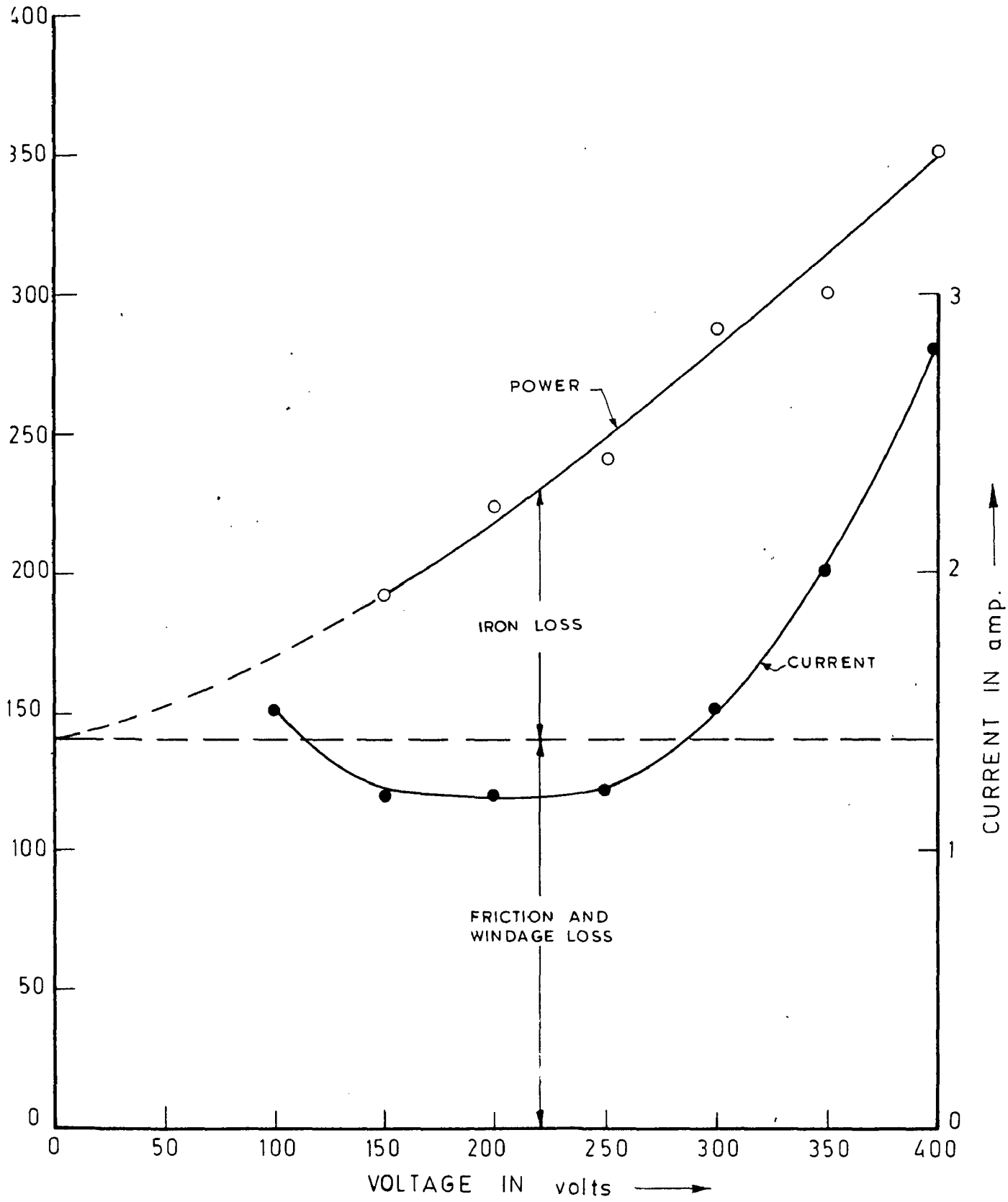

FIG. 9(a) NO LOAD TEST

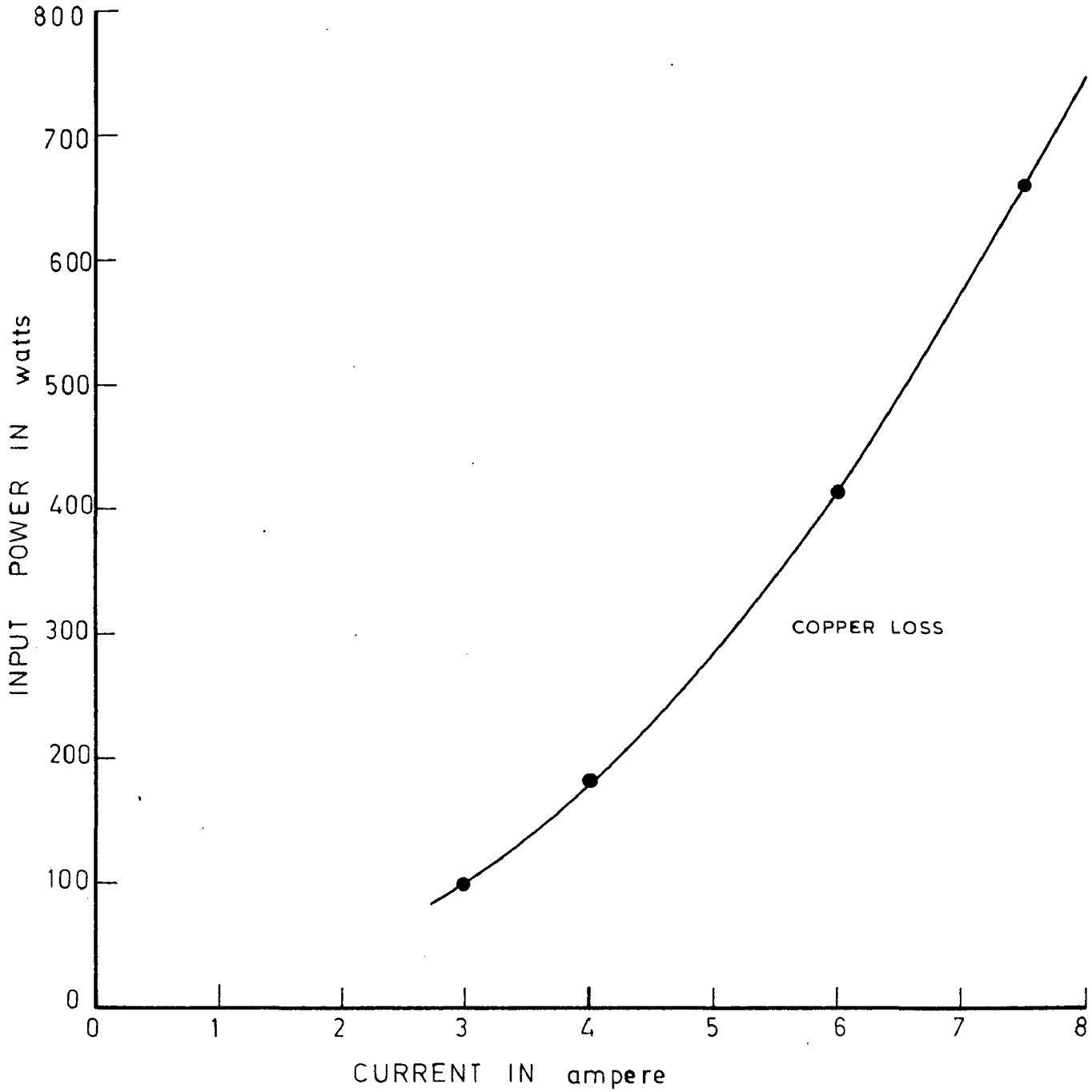

FIG. 9(b) SHORT CIRCUIT TEST

CHAPTER IV

A [illegible] MEASUREMENT FOR THE MEASUREMENT OF HOT-SPOT [illegible] ELECTRICAL MACHINES

This chapter deals with an experimental method which has been developed for accurate and precise measurement of temperatures at hot-spots in a electrical machine. This method can be used for the measurement of temperature in both stationary and rotating parts of the machine. The temperature sensors are fitted at various spots whose temperature are to be measured.

4.1 SELECTION OF TEMPERATURE SENSOR FOR MEASUREMENT

Several types of temperature sensing elements are available which can be used to measure the temperature. The details of these elements are given in tabular form in table Some details of those elements which can be used for electrical machines temperature estimates are discussed below

(i) Thermocouple — Thermoelectric sensing elements are used in thermocouple circuits. A basic thermocouple, consists of a pair of wires of different metals which are joined at two ends :- One end is used for sensing the unknown temperature and is called (sensing junction) and the other end is maintained at some fixed or reference temperature and is called reference junction. When temperature difference exists between the sensing junction and the reference junction, an electromotive force is produced which causes current to flow through the circuit. This thermoelectric effect is also known as seebeck effect.

(2) Thermopile – It is combination of several thermocouples of the same material connected in series. The output of a thermopile is equal to the output from each thermocouple multiplied by a number of thermocouples in the thermopile assembly. All reference junction must be at the same temperature.

(3) Resistive sensing element – Resistive temperature sensing elements are conductors and semiconductor which change their resistance with the change in temperature. Conductors which are used for this purpose are discussed below:

Platinum wire element : These are used for laboratory work, (range -190°C to + 630°C)
mobile, and space instrumentation and for industrial measurement when special requirement for accuracy exist.

Nickel wire element : These are less costly than platinum wire.
(-100°C to + 300°C)
These are commonly used in transducers for industrial and commercial applications.

Tungsten wire element : They compare in cost with platinum element but are more difficult to manufacture, primarily because of the high temperature required for their annealing and their brittleness resulting from this necessary process.

Copper wire element : Elements wound from copper wire were frequently used in the past. Resistance vs Temperature characteristics show an unusually good linearity, but their low resistivity requires the use of impractically long lengths.

Metal film element : Metallic film deposited on insulating material, such as platinum on ceramic, have been used successfull

for temperature measurement. The resistance Vs temperature relationship of such sensing elements is empirical i.e., it must be determined from experimental data since no theoretical relationship has been established.

Semiconductors : Germanium crystals and silicon crystals are used for liquid-hydrogen temperature measurement. Germanium crystals have high negative temperature coefficient of resistance. Their resistance Vs temperature characteristic is non-linear. While silicon crystal have high positive temperature coefficient of resistance.

Thermistors are also semiconductor materials whose resistance vary with change in temperature.

Carbon resistors : They are used below 60 K. Their behavior is similar to that of semiconductors. They are having high resistivity and low temperature coefficient of resistance. Disadvantages encountered in their use are their sensitivity to pressure variations when used in pressurised units or tanks, long term drifts in their resistance, relatively long response time.

b.2 BASIC PRINCIPLE

In this method thermistor has been used as a temperature sensing device. Thermistor is connected in an oscillator circuit with the variation in temperature, the resistance of thermistor changes. This change in resistance varies the frequency of oscillator. Large number of sensors can be fitted at different appropriate points in the machine where hot spots are expected. From stationary part of the machine, the signals can be directly given to measuring circuits. From rotating part of the machine,

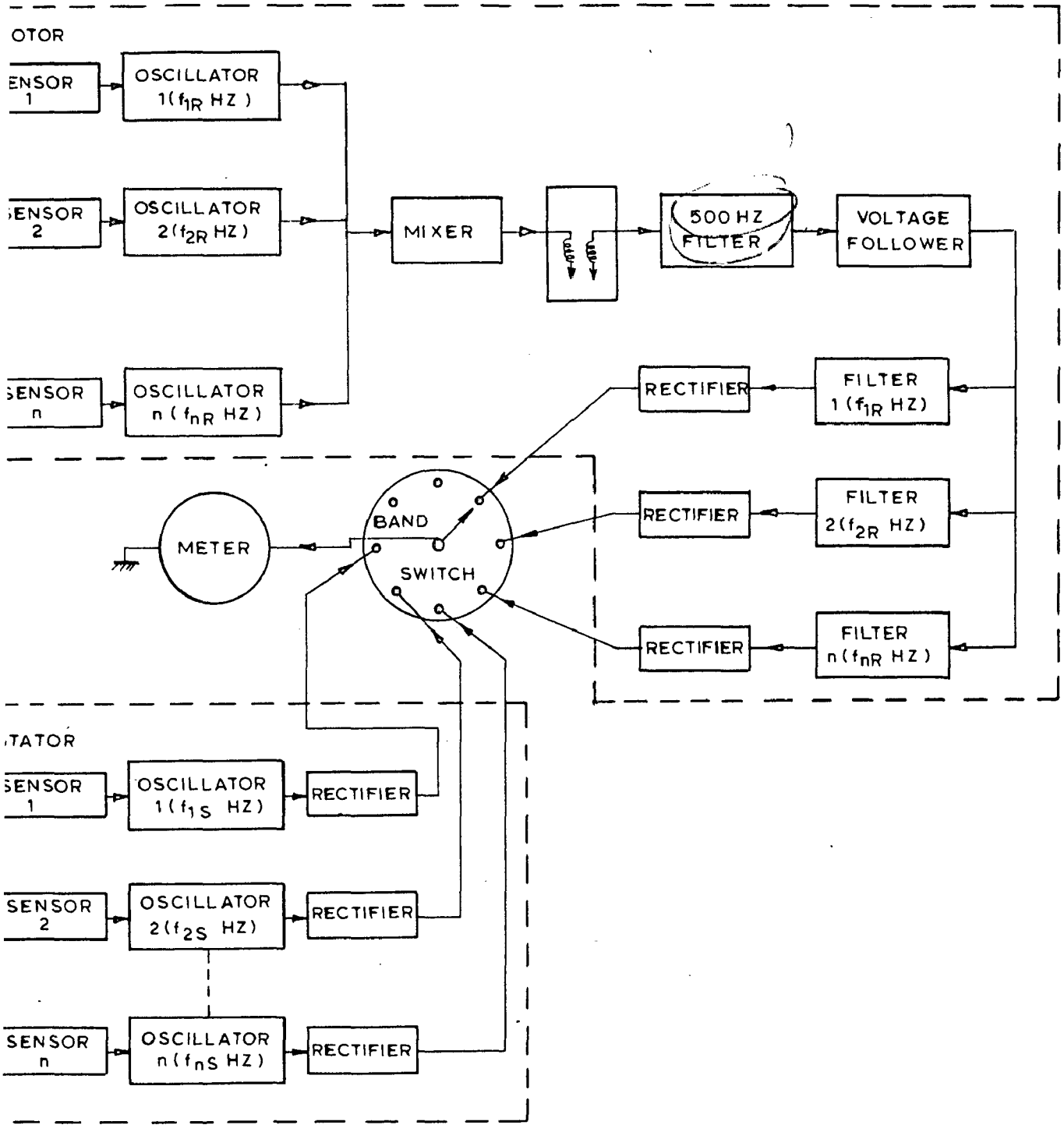

FIG. 10 _BLOCK DIAGRAM

the signals are to be telemetered after proper processing. This complex frequency have obtained after telemetering is then passed through different filter circuits for separating out the original signals of various input oscillators. Filters are specially designed corresponding to each oscillator circuit. These frequency signals are measured after further processing of the signal either by analog meters or recorders.

b.3 TEMPERATURE SENSOR : Fig.10 shows the complete temperature measuring scheme in block diagram form. It consists of temperature sensors, oscillators mixer, telemetring transformer, High pass filter, Band pass filters rectifiers and analog meters.

Thermistors : This is a semiconductor which show resistance change with slight change in temperature. They are made of ceramic and usually mixtures of sulfides, selenides or oxides of manganese nickel and cobalt copper, iron uranium. The materials are calcined blended, formed into desired shape and fired into a hard ceramic form. It is possible to form very thing beads.

Till now different types of sensors have been discussed. Out of them we have selected thermistors as sensor for this scheme because they are small, robust and can be used with either a.c. or d.c. They have a rapid response to change in temperature and, provided they have been pre-aged by exposing to a temperature slightly higher than to which they are to be subjected, they are very stable. They can be used from -60°C to 300°C but the upper limit is about 150°C and the accuracy is ± 0.01°C at 100°C.

The resistance temperature relationship of the thermistor is exponential, and varies according to the relationship $R_t = R_0 e^{\beta\left(\frac{1}{T} - \frac{1}{T_0}\right)}$

where,

R_t = Temperature at T°C

R_{t_0} = Temperature at T°C

β = Temperature coefficient

e = 2.71828

Thermistors have high temperature coefficient of resistance. They are of two types —

(1) Positive temperature coefficient thermistor (P.T.C)

(2) Negative temperature coefficient thermistor (N.T.C)

Particular thermistor used in this set-up is have negative temperature coefficient. We have selected this because it has been available for some 25 years, is well established in circuit applications, particularly those where an analytical solution of the circuit problem is desirable. This is because the resistance-temperature dependence can be specified fairly closely by an exponential function. With N.T.C. thermistors there is also no problem with regard to non-linear electrical behavior at the contacts.

Commercial P.T.C. thermistors are commercially new, can not be specified precisely for analytical work and have a temperature coefficient of resistance which depends markedly on temperature. However over limited ranges of temperature can be very large with consequent system gain in control applications

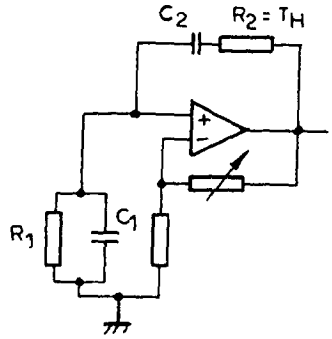

OSCILLATOR

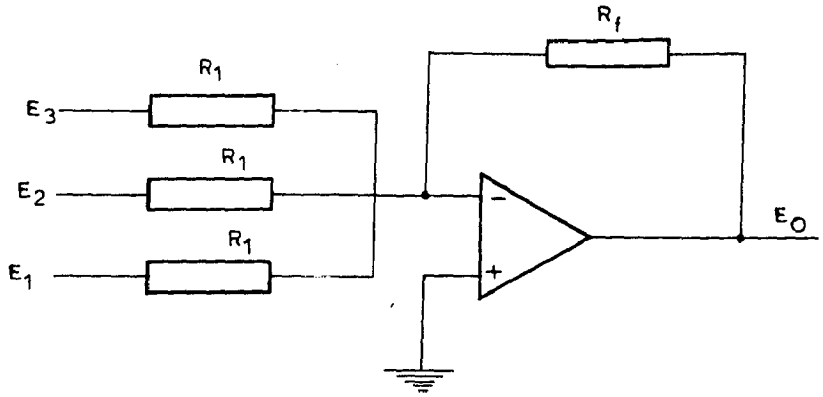

$$E_O = -\frac{R_a}{R_1}[E_1 + E_2 + E_3]$$

MIXER

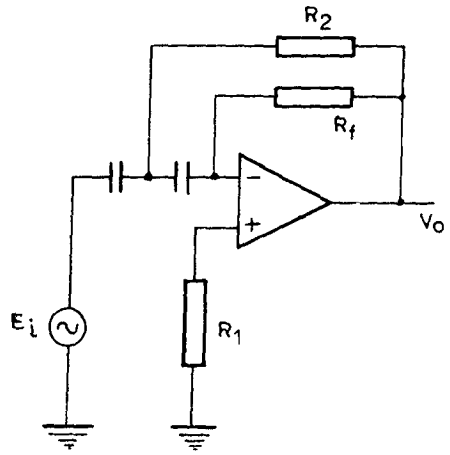

HIGH - PASS FILTER

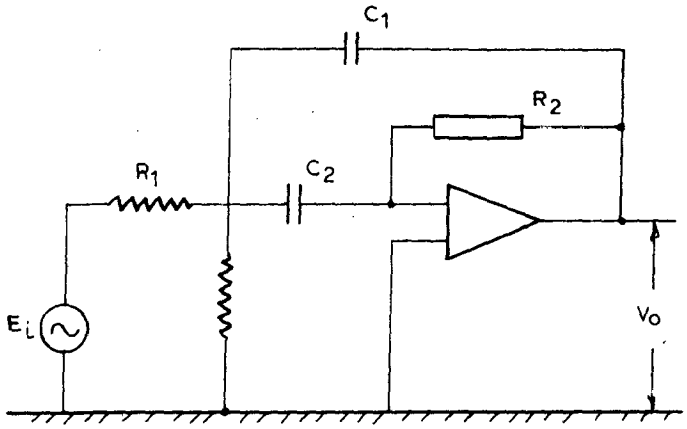

NARROW - BAND BAND - PASS FILTER

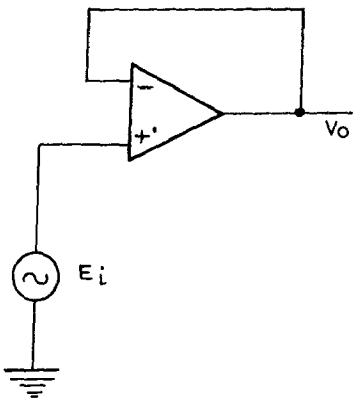

VOLTAGE FOLLOWER

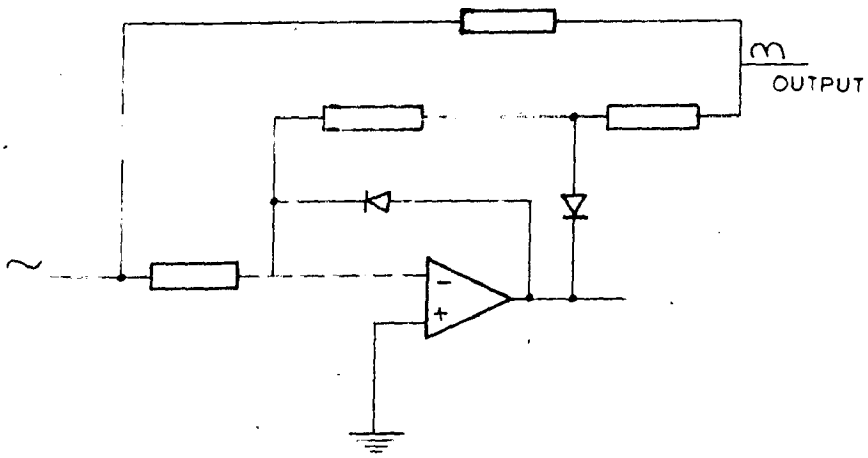

RECTIFIER

FIG. 11 - CIRCUIT - DIAGRAM

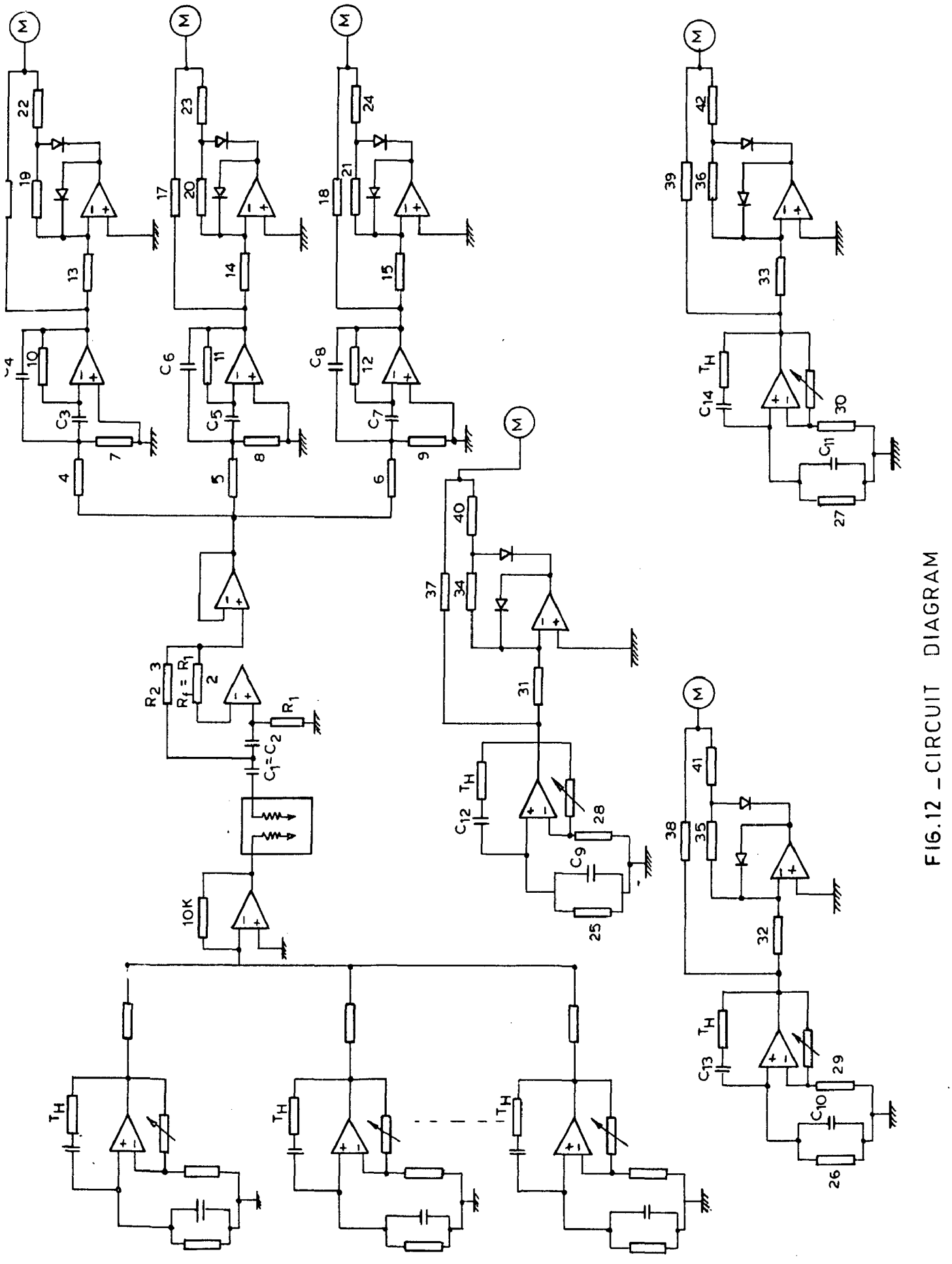

FIG.12 _CIRCUIT DIAGRAM

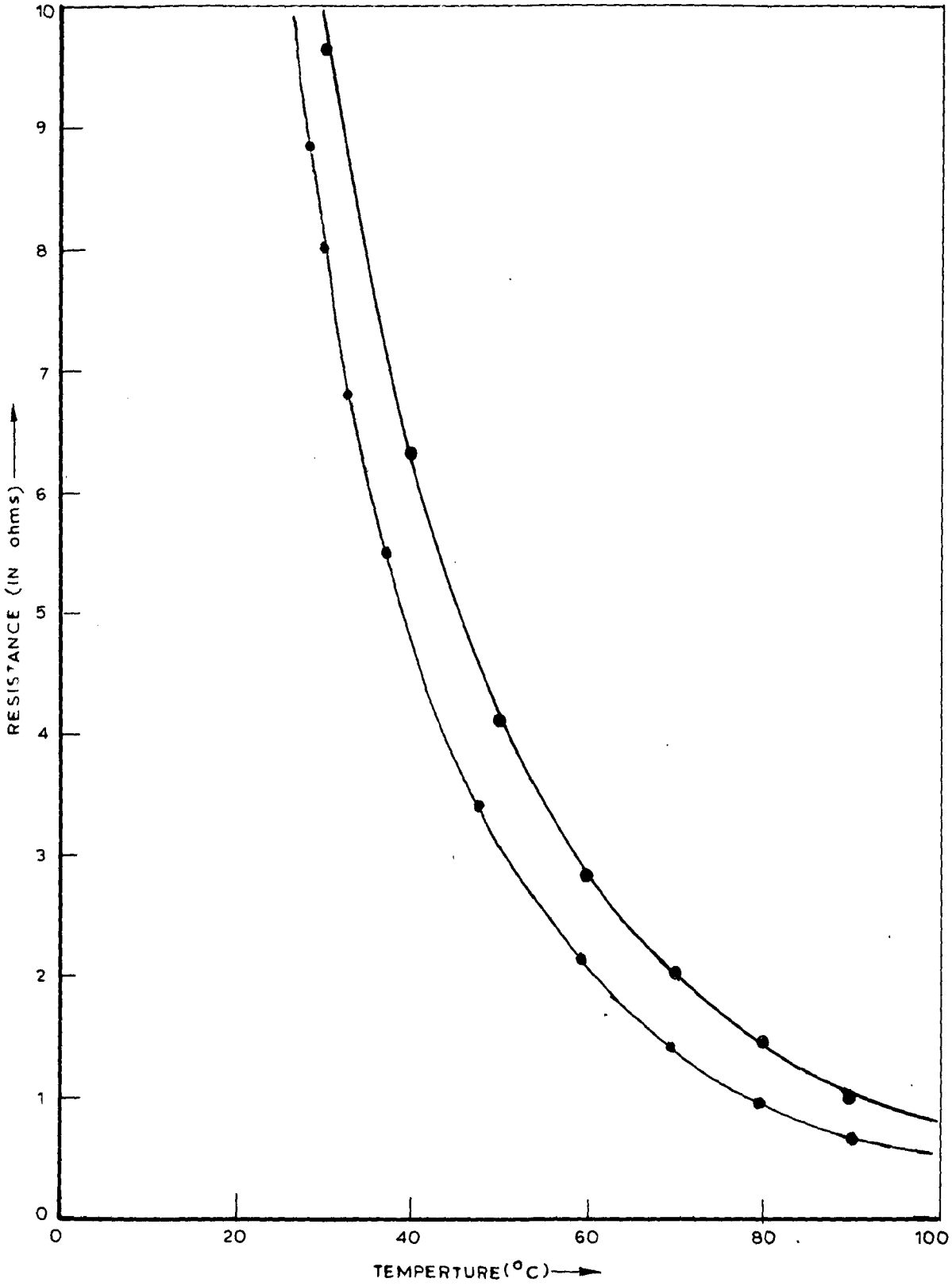

FIG. 13 _THERMISTOR CHARACTERISTIC

The characteristic of two (N-C) thermistor having resistance (1) 3.6 K ohm (2) 3.8 K ohm at 30°C is shown in Fig.13.

Oscillator : The circuit diagram of the wein bridge oscillator is shown in Fig.11. Oscillation frequency can be adjusted by changing the value of resistance R_2 and capacitance C_1 and C_2. The frequency of oscillator, f is computed by the relation

$$f = \frac{1}{2\pi\sqrt{R_1 R_2 C_1 C_2}} \qquad (1)$$

where R_1 and R_2 are resistance and C_1 and C_2 are capacitance of different value. R_1 and C_1 are connected in series and R_2 and C_2 are connected in parallel. R_1 and C_1 are in the feedback loop of the operational amplifier. The diode D_1 and D_2 are connected for wave shaping. The amplitude of the waveform is adjusted by the preset.

If resistance R_1 and R_2 and capacitance C_1 and C_2 are equal then,

$$f = \frac{1}{2\pi RC}$$

where $R_1 = R_2 = R$

$C_1 = C_2 = C$

Thermistor which is used for sensing the temperature is placed in place ofresistance R_1 in the feedback path of the circuit. The thermistor is having resistance of 10 K ohm at room temperature (25°C). The resistance of thermistor can be

The characteristic of two (N.C) thermistor having resistance (1) 3.6 K ohm (2) 3.9 K ohm at 30°C is shown in Fig.13.

Oscillator : The circuit diagram of the wein bridge oscillator is shown in Fig.11. Oscillation frequency can be adjusted by changing the value of resistance R_2 and capacitance C_1 and C_2. The frequency of oscillator, f is computed by the relation

$$f = \frac{1}{2\pi\sqrt{R_1 R_2 C_1 C_2}} \qquad (1)$$

where R_1 and R_2 are resistances and C_1 and C_2 are capacitances of different values. R_1 and C_1 are connected in series and R_2 and C_2 are connected in parallel. R_1 and C_1 are in the feedback loop of the operational amplifier. The diodes D_1 and D_2 are connected for wave shaping. The amplitude of the waveform is adjusted by the preset.

If resistance R_1 and R_2 and capacitances C_1 and C_2 are equal then,

$$f = \frac{1}{2\pi RC}$$

where $R_1 = R_2 = R$

$C_1 = C_2 = C$

Thermistor which is used for sensing the temperature is placed in place ofresistance R_1 in the feedback path of the circuit. The thermistor is having resistance of 10 K ohm at room temperature (25°C). The resistance of thermistor can be

found out at different values of temperatures either by using resistance temperature curve or by heating the thermistor and noting down the resistance. The resistance Vs temperature characteristic for the used thermistor is shown in table). The oscillator frequency for different values of resistance R_1, at different temperature can be calculated. This will give the variation in frequency of oscillator at the entire desired temperature range. The temperature variation may be from ambient temperature (25°C) to higher than 90°C. So thermistor resistance corresponding to these temperatures are 10 K ohm and 830 ohm respectively.

Three rotor hot-spot points and three stator hot-spot points are considered for designing the oscillators. The three rotor points are at slot, overhang and the core. Similarly, three stator points are also at slot, overhang and the core.

The frequencies of the oscillator for the rotor are chosen as 2000 Hz, 11000 Hz and 20000 Hz respectively. The capacitors are chosen of the same value i.e. $C_1=C_2=C=0.01 \times 10^{-6}$ Farad. After substituting the values of C_1, C_2, R_1 and f for the three cases, the corresponding values of R_2 is found out as 60.25 K ohm for 2000 Hz oscillator, 2.97 K ohm for 11000 Hz oscillator and 0.305 K ohm for 20000 Hz oscillator.

Oscillators for stator portions are designed for frequencies 200 Hz, 400 Hz and 600 Hz. In this case capacitors are chosen of same value i.e. $C_1 = C_2 = C = 0.1 \times 10^{-6}$ Farad, the thermistor resistance at 45°C is 4100 ohms. The oscillator resistance R_2 is found out as 15.46 K ohm for 200 Hz frequency oscillator, 3.86 K ohm for 400 Hz frequency oscillator and

1.71 K ohm for 600 Hz frequency oscillator.

Mixer: An adder circuit has been used as a mixer which is shown in Fig.11. The output of the various oscillators are connected to the input point of the adder. The capacitors in the circuit have been used for d.c. oscillation.

High pass filter : The circuit diagram of a high pass filter is shown in Fig.11. This circuit is designed as a high pass butterworth filter with a roll-off of 40 db-decade below the cut-off frequency v_0. The following is the design procedure of high pass filter –

(i) Choose a cut-off frequency v_0 or f_0

(ii) Let $C_1 = C_2 = C$ and choose a suitable value

(iii) Calculate R_1 from the relation $R_1 = \frac{1.414}{v_0 \pi C}$ (2)

(iv) $R_2 = \frac{1}{2} R_1$

(v) To minimise d.c. effect let $R_2 = R_1$

This filter is used to suppress 50 Hz supply frequency. Since the supply frequency is superimposed on the achieved signal waveform which is received from rotor. Actual waveform is obtained after high pass filter.

For the filter design, cut-off frequency is chosen as 500 Hz. The capacitor values are selected as $C_1 = C_2 = C = 0.022 \times 10^{-6}$ Farad. After substituting these values in equation (2) the value of R_1 is obtained to be 20.5 K ohm. Now the value of R_2 will be equal to half of R_1 value. So $R_2 = \frac{1}{2} R_1 = 10.25$ K ohm

Voltage Follower : The circuit of voltage follower is shown in Fig.11. It is also called as a source follower, unity gain amplifier, buffer amplifier or isolation amplifier.

The input voltage, V_i from the previous stage is applied directly to the positive input. Since the voltage between positive and negative pins of the operational amplifier can be considered zero, so the output voltage will be $V_o = V_i$. Note that the output voltage equals the input voltage in both magnitude and phase. So the name of the circuit implies, the output voltage follows the input or source voltage. The voltage gain is unity.

The input impedance looking into the positive input terminal is very high i.e. of the order of several megohms.

Design of Wide-Band Band-Pass Filter : By appropriately choosing the value of, the circuit shown in Fig.11 can be designed as either a wide-band filter ($Q<10$) or as a narrow band filter ($Q>10$). Unlike the low-pass or high-pass filters of section the filter can be designed for a closed loop gain greater than 1. The maximum gain, A_p, occurs at resonant frequency. For this ω_p and Q are chosen and the bandwidth B is calculated. To simplify the design and reduce the number of calculations the capacitors are chosen as $C_1 = C_2 = C$. The values of the resistances of the circuit are calculated by the following relation

$$R_2 = \frac{Q}{B\omega_p} \qquad (3)$$

$$R_1 = \frac{R_2}{A_p} \qquad (4)$$

$$R_3 = \frac{R_2}{4Q^2 - 2A_f} \qquad (5)$$

R_3 will be positive for, $4Q^2 > 2A_f$

From Fig.7 it can be seen that as the temperature changes from 29°C to 100°C resistance of thermistor changes from 10 K ohm to 500 ohm. Hence frequency obtained from wein bridge oscillator will have large band width B and hence Q can be calculated with the help of following equation

$Q = \frac{\sqrt{F}}{B}$; A_f is taken as 1. The capacitor value is chosen as $C = 0.02 \times 10^{-6}$ Farad in present case. By substituting the value of B and C in equation (3) the value of R_2 is found out. By substituting R_2 and A_f in equation (4), R_1 is calculated. Then finally by substituting R_2, Q and A_f in equation (5), the value of R_3 is found out. Table-1 shows the various parameters of different filters.

$= 0.022 \times 10^{-6}$ Farad)

Frequency range for temperature 25C to 100°	B	Q	R_2	R_1	R_3	A
(1) 1000 Hz to 3000Hz	2000	1	7.2 K ohm	2.4 K ohm	7.2 K ohm	1.5
(2) 10500Hz to 12500Hz	3000	3.6	4.8 K ohm	240 ohm	150 ohm	10
(3) 19000Hz to 22000Hz	3000	6.6	4.8 K	240 ohm	33 ohm	10

Rectifier : Fig.11 is a circuit diagram of high precision rectifier. The signals of quite low value like 0.2 mV can be rectified by this type of rectifier. In these circuits rectification is achieved without sacrificing a significant portion of the signal

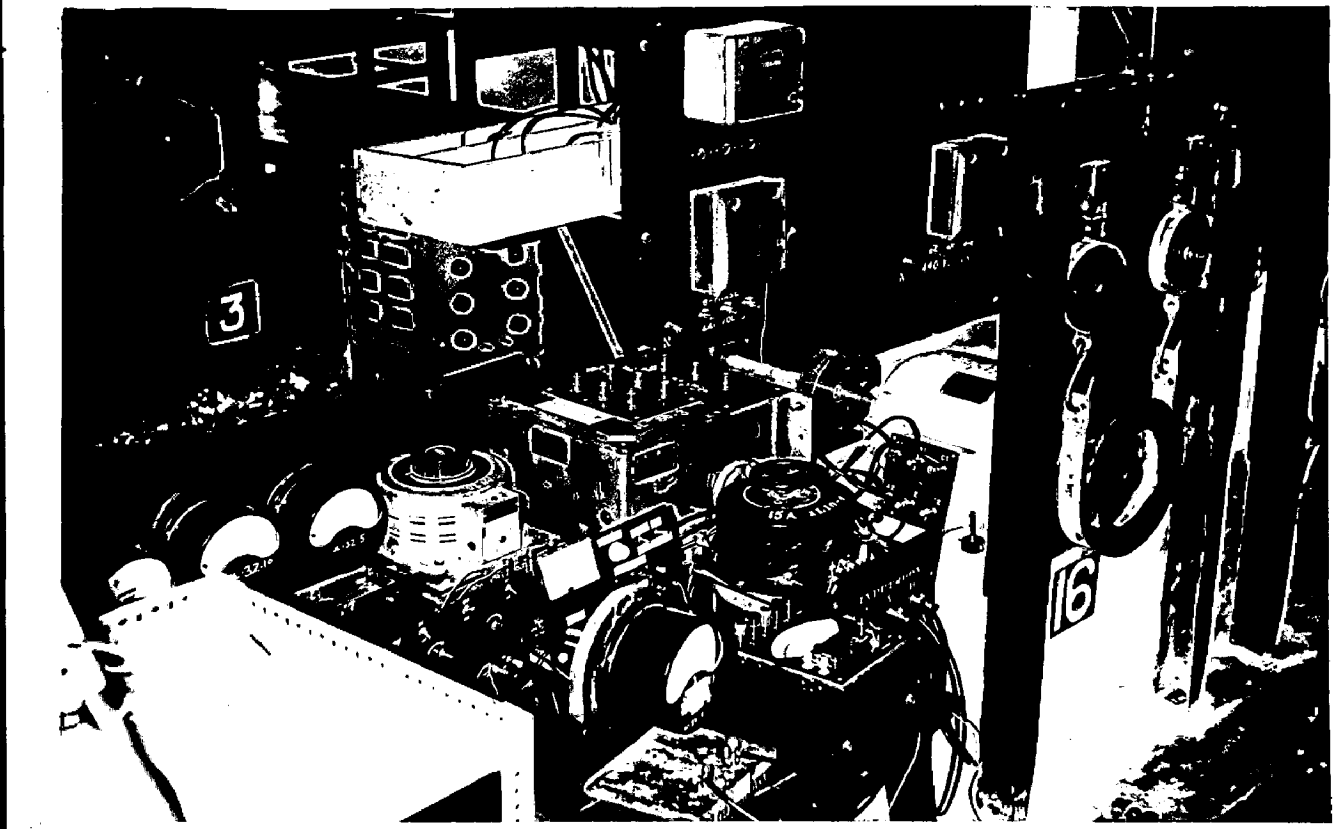

Photograph 1 COMPLETE EXPERIMENTAL SET-UP.

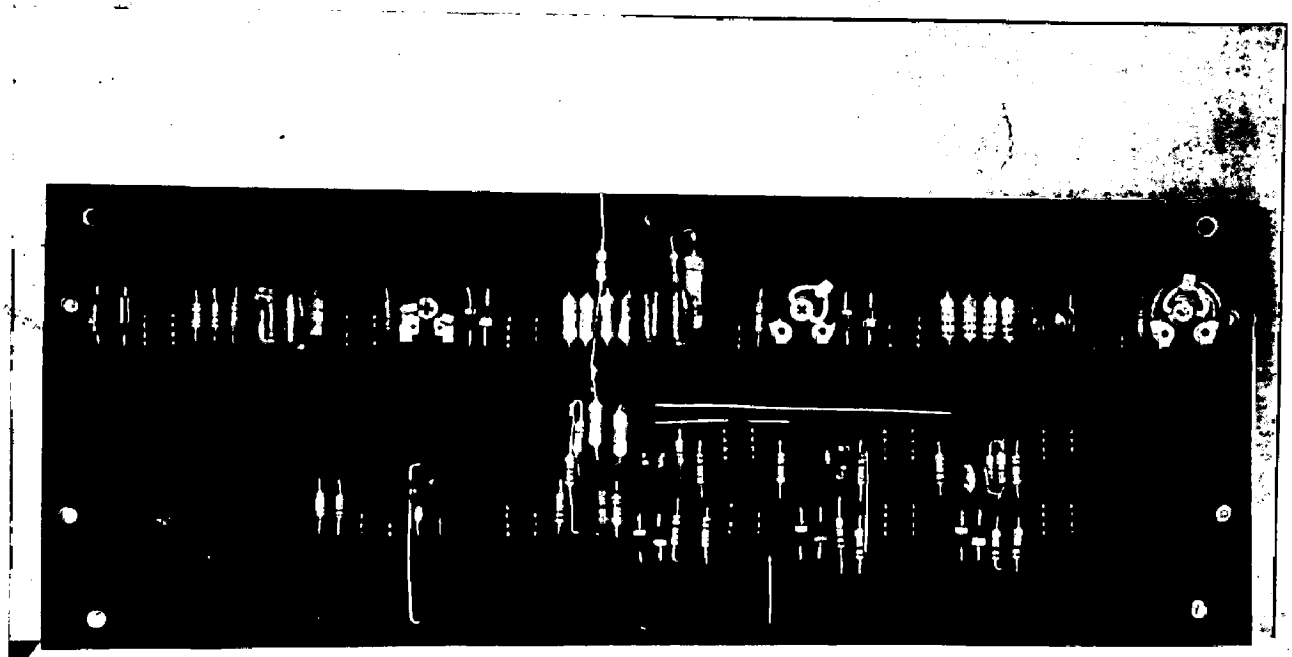

Photograph 2 PLACEMENT OF VARIOUS ELECTRONIC COMPONENTS IN THE SYSTEM.

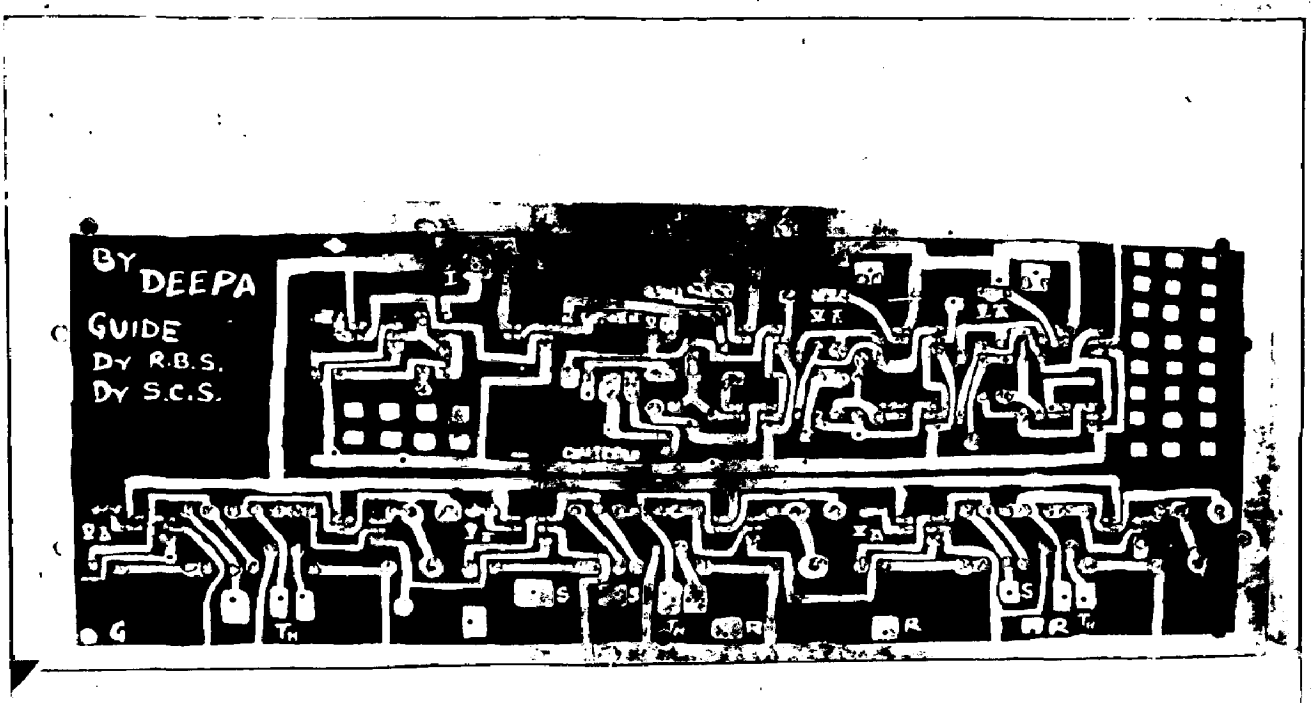

Photograph 3 PRINTED CIRCUIT BOARD FOR ELECTRONIC COMPONENTS.

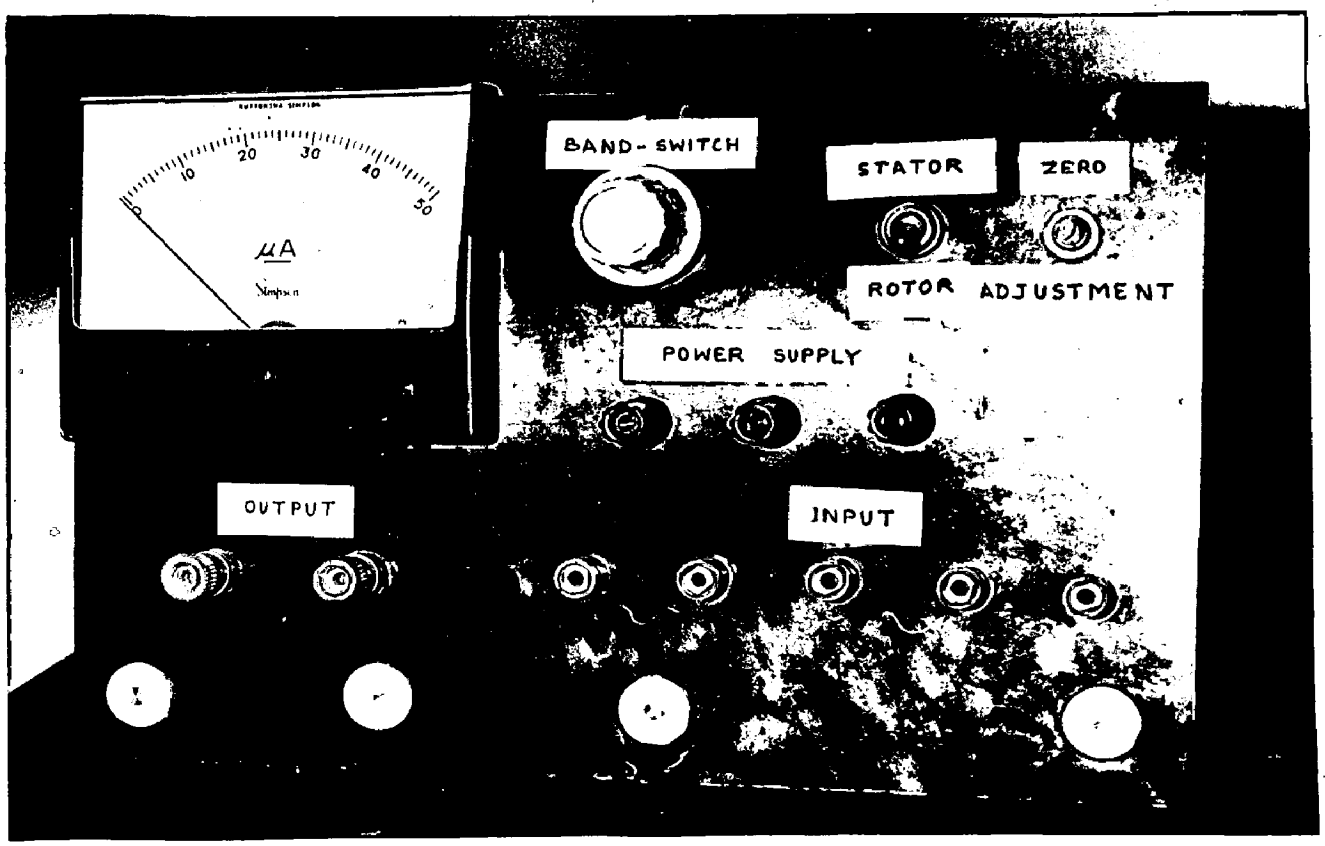

Photograph 4 FRONT-PANNEL.

Photograph 5 EMBEDDING OF THE EMITTOR IN ROTOR.

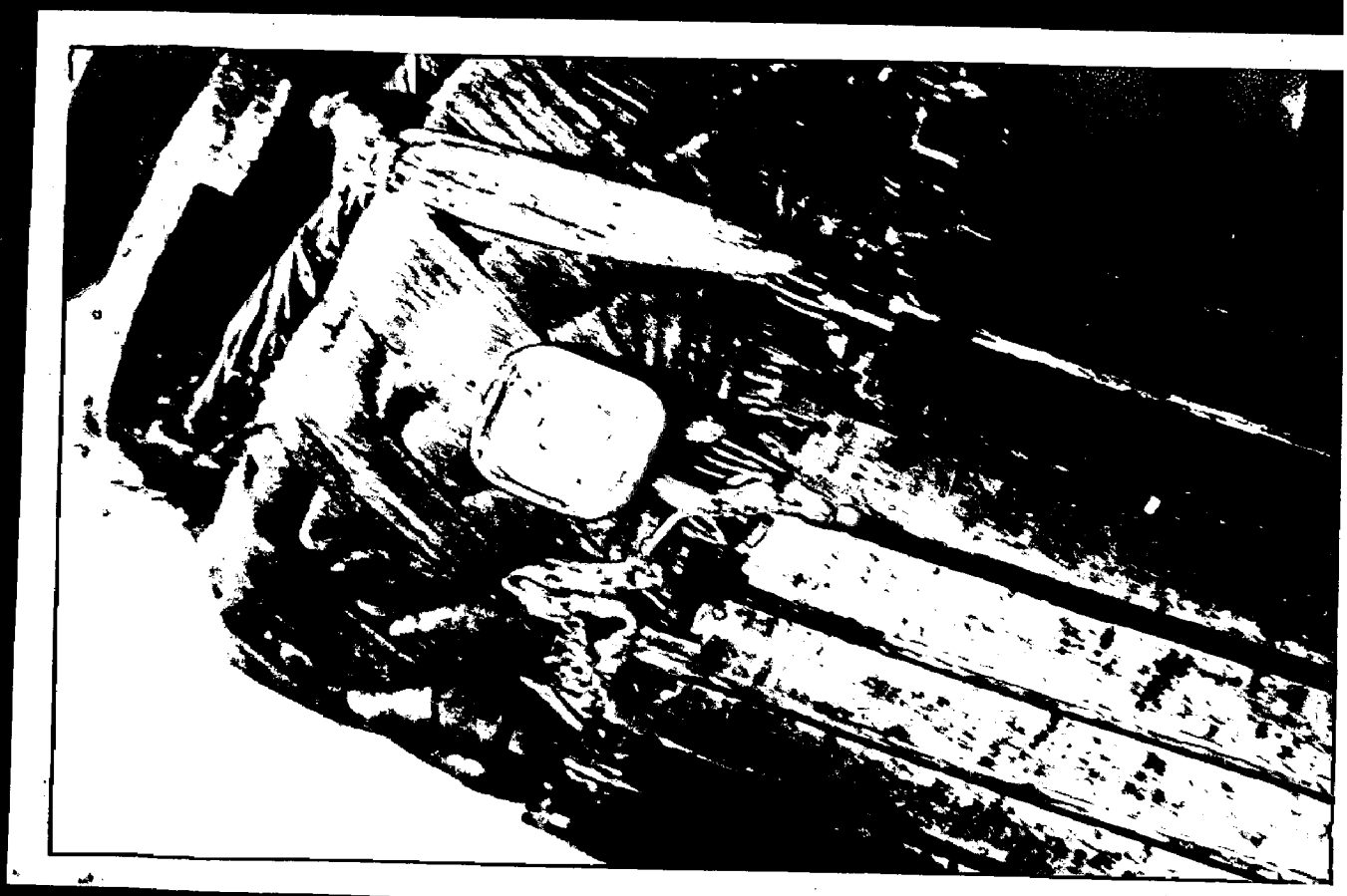

Photograph 6 EMBEDDING OF THE EMITTOR IN ROTOR.

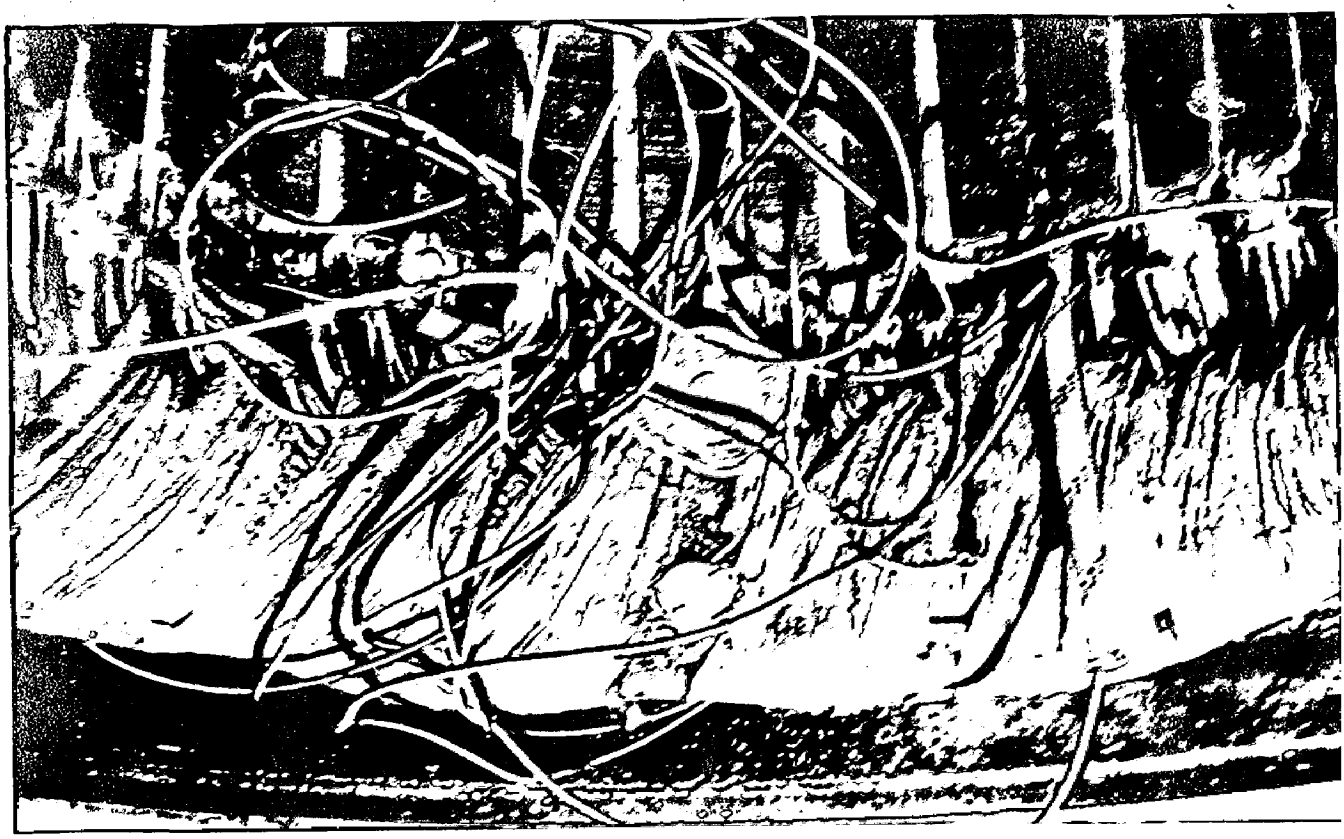

Photograph 7 [illegible] OF THE PISTON IN STATOR.

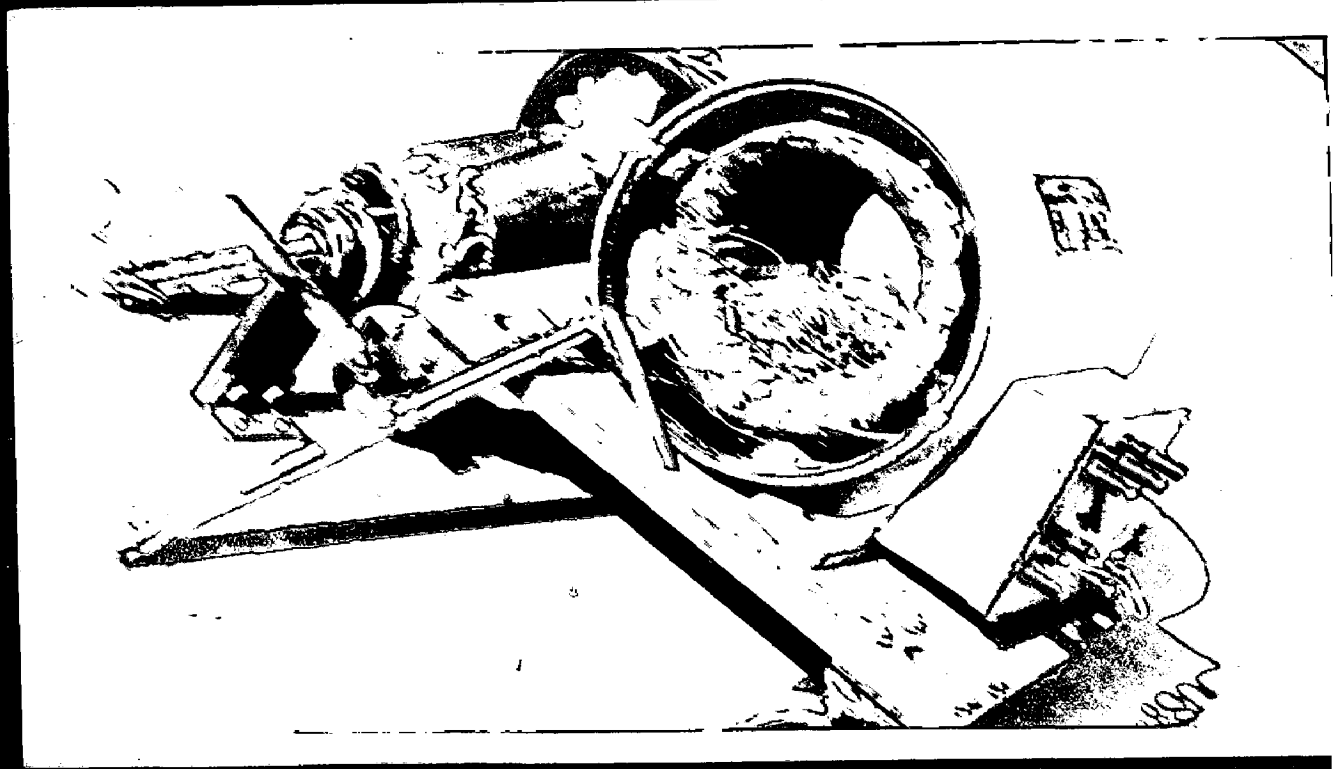

Photograph 8 STATOR, ROTOR AND CHART [illegible].

to forward bias rectifying diodes. Since the diodes are in the feedback loop of an amplifier. The feedback drives the diodes into and out of conduction for only very small input signal changes, permitting rectification of millivolt level signals.

Rectifier is designed for unity gain and hence all the resistances are made equal to 10 K ohm and ordinary diodes are used for design purpose.

Telemetring Transformer: Fig.12 shows the complete circuit details of the instrumentation scheme. The signal is transmitted from rotor to stator by using induction phenomena. The supply to the rotor circuit is also transmitted by using transformers.

4.4 EXPERIMENTAL SET-UP

Photograph 1 shows the complete experimental set-up. A 3-phase, 5 H.P., 7.5 Amp. Induction motor has been used in this experiment. Three resistors which are placed near the single phase auto transformer measure line currents.

The temperature measuring electronic circuit for stator points and also for rotor points (after telemetry) along with its power supply is placed before the auto-transformer. Photograph 2 shows the placement of various electronic components in the system The printed circuit for the electronic system is shown in photo-graph-3. Photograph-4 shows the details of the front-panel of the measuring unit. The microammeter gives the final deflection proportional to temperature of the hot-spot which is connected to it via band switch. The hot-spot temperatures of different points can be seen on the analog meter by connecting them respectively

with the help of band switch. The bandswitch is located by the left hand side of the analog meter. This bandswitch is having six points i.e. three for rotor and three for stator. The bandswitch is connected to stator or rotor points by a toggle switch which is located near the bandswitch. The zero-adjustment potentiometer is shown in the extreme left top of the photograph. Two points of the meter are shown as output points which can be used for recording purpose. The recorder can be directly connected to those points. The power supply point for the measuring circuit are shown in the middle of the front board.

Photograph 5 and 6 shows the embedding of thermistors in the rotor overhang and rotor slot. The 5 n.p. coin is placed near the thermistors to have an idea about their size. The two points of the thermistor are taken out for further connections through insulated leads. Photograph-7 shows the location of thermistors at the various points on the stator. The thermistors are embedded in the stator slots, stator overhang and stator core.

Photograph-8 shows the stator and rotor (both placed seperately after opening) with embedded thermistors. This figure also shows the extension of the shaft which has been done for monitoring the rotor temperature measuring circuit (before telemetry) and for telemetring the signal.

6.5 INSTRUMENTATION

The instrumentation scheme was tested for block rotor condition and also for the loaded condition of the electrical machine.

Block Rotor Test :

The motor is connected to a 3-phase supply by means of star connections through 3-phase autotransformer. Rotor of the machine is blocked by means of a bolt. Observations are made for time Vs frequency for rotor points till steady state is reached. These frequencies are noted after filter circuits. For stator points readings are taken time Vs meter reading. Observations are given in table-I both for Rotor and Stator.

Calibration is done by placing the resistance in place of thermistor. Observations are made Resistance Vs Meter Reading for stator (Fig.1,4) and Resistance Vs frequency for Rotor (Fig.15). A plot has already been made for Resistance Vs temperature (Fig.16) for thermistor. With the help of Figures (14,15) the final plot Temperature Vs Time is obtained.

Load Test :

For this case load is taken as 5 Ampere. Observations are taken time Vs Meter reading. These values are given in table I For calibration temperature Vs Meter reading Fig.(17) is taken (see table-4). For this, thermistor is placed in hot chamber these temperature is observed with the help of a thermometer. Plot between Temperature Vs Time is obtained (Fig.18).

Result Analysis : Block Rotor Test Steady State Temperature :-

Stator Core Temperature = 62°C

Stator Slot Temperature = 71°C

Stator winding temperature = 100°C

Rotor core temperature = 65°C

Rotor slot temperature = 90°C

Load Test

Steady State Temperature :-

Stator core temperature = 57°C

Stator overhang temperature = 60°C

Time	Heater						Boiler						
	Core		Overhang		Hot		Hot		Hot	Time	Core		
	Volt.	Temp. °C	Volt.	Temp. °C	Volt.	Temp. °C	Volt.	Pressure lbs	Temp. °C		Volt.	Frequency lbs	Temp. °C
0	23	25	24	25	30.5	25	33.5	1.76		0	15	12.77	25
3	26.5	39	25	36	31.5	37	32.5	1.64		2	16	11.65	26
6	26.5	35	23	45	32.5	44	31.0	1.55		3	19	11.35	30
10	27.0	39	29.5	57	33	43	-	-		5	20	11.11	32
12	29.0	45.5	30	63	33.5	53	31	1.52	50	5	22	10.85	33
20	29	55.5	30.5	01	33.5	53	30.25	1.57	57	7	23	10.85	34
25	29	55.5	30.5	01	33.5	53	28.25	1.57	57	9	24	10.85	34
30	29	55.5	30.5	01	33.5	53	27	1.60	63	11	25	10.11	35
35	30	57	30.5	01	33.5	53	27	1.64	70	15	25	10	37
40	30.5	62	31.0	00	35	70	27	1.65	75	16	27.5	10	40
45	30.5	62	31.5	100	35.5	76	25.5	1.72	82	20	20	10	40
50	30.5	62	31.5	100	35.5	76	26.5	1.72	02	25	30	9.71	43
60	30.5	62	31.5	100	35.5	76	25	1.76	90	27	31	9.72	44
70	30.5	62	31.5	100	35.5	76	25	1.76	90	30	31	9.77	44
80	30.5	62	31.5	100	35.5	76	25	1.76	90	31	31	9.65	45
										31	31	9.65	45
										31	32	9.65	45
										31	32	9.65	45
										32	32	9.65	45

Calibration

Resistance	Stator			Rotor			
	Core	Overhang	Slot	Slot		Core	
	M.P.	M.P.	M.P.	M.P.	Reactance Ohms	M.P.	Reactance Ohms
10.2	-	-	-	-	-	12	13.16
10 K	25	24.5	30.25	34	1.22	16	12.35
9 K	25.75	25	30.75	-	-	20	11.16
8 K	-	-	-	-	-	23	11.17
7 K	26.5	26	31.0	31.5	1.33	25.5	10.53
6 K	-	-	-	-	-	28.5	10.00
5 K	27.5	27.5	32.0	30	1.45	31	9.71
4 K	-	-	-	-	-	32.5	9.45
3 K	29.5	29.0	33.5	28	1.55	32.5	9.45
2 K	30.5	30.0	34.5	-	-		
1 K	31.5	30.5	36.0	25.5	1.70		
700 ohm	32.0	31.0	36.5	25.0	1.77		
500 ohm	32.0	31.5	37.0	25.0	1.77		

Table 1

LOAD TEST VOLTAGE 400 V, Load 5 Amp.

Time Minutes	Stator			
	Core		Overhang	
	M.R.	Temp. °C	M.R.	Temp °C
0	0	29	18.5	29
7	17	30	19.5	34
15	19	32	20	35
20	21	35.5	22	38
30	22	38	22.25	44
40	23.25	46.5	24.25	60
50	24	53.5	24.25	60
70	24.25	57		
80	24.25			

Table 4

Calibration for Load Testing

Temp	Core	Overhang
32°C	17.25	19
35°C	20.75	20
38°C	22	21.5
45°C	23	22
50°C	23.75	22.75
53.5°C	24	23.75
60°C	24.5	24
65°C	25	24.25
70°C	25.25	25
75°C	25.25	25.5
80°C	26	25.75
85°C	26	26.25
90°C	26	26.25

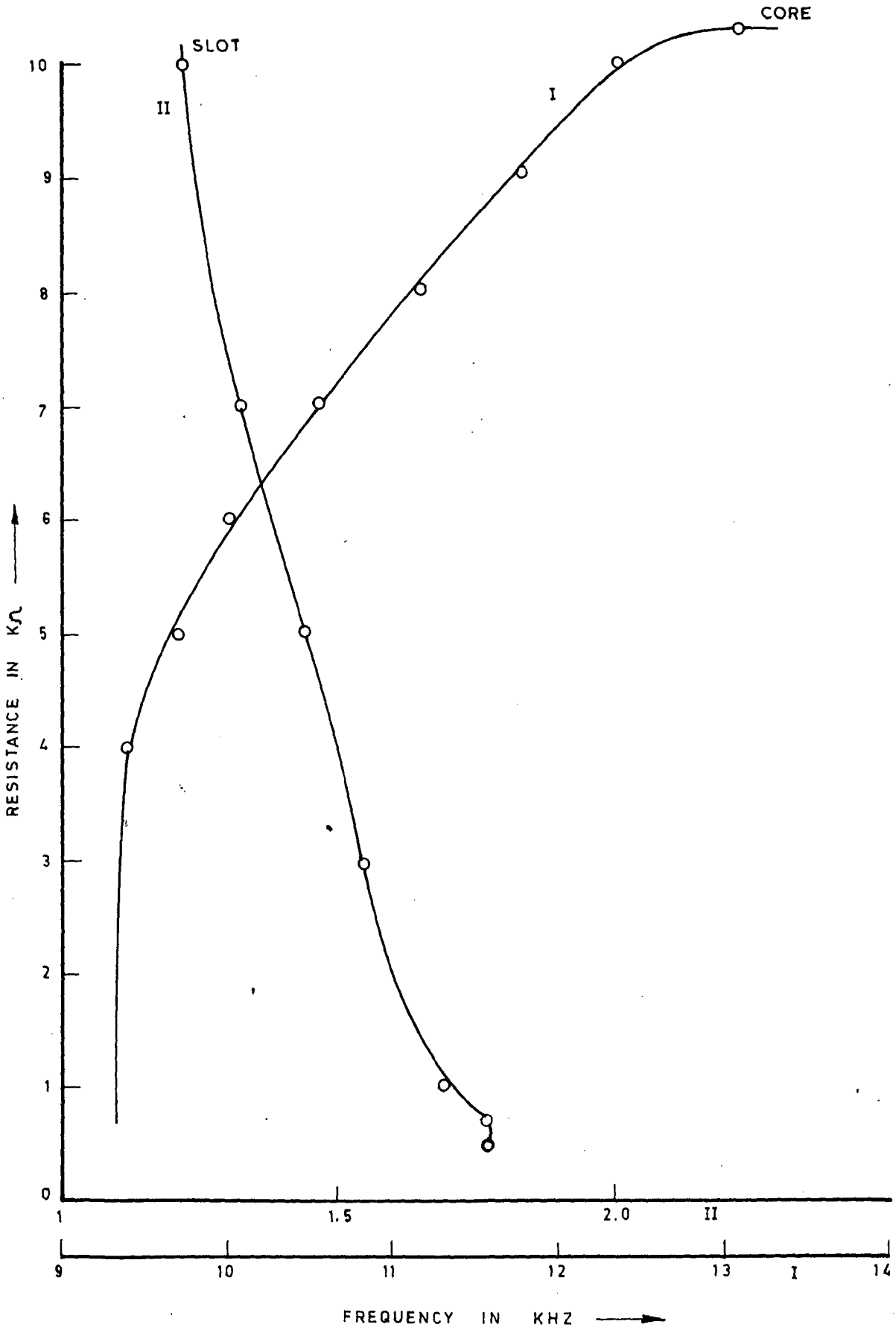

FIG. 14 _ BLOCK ROTOR TEST CALIBRATION CURVE FOR ROTOR POINTS

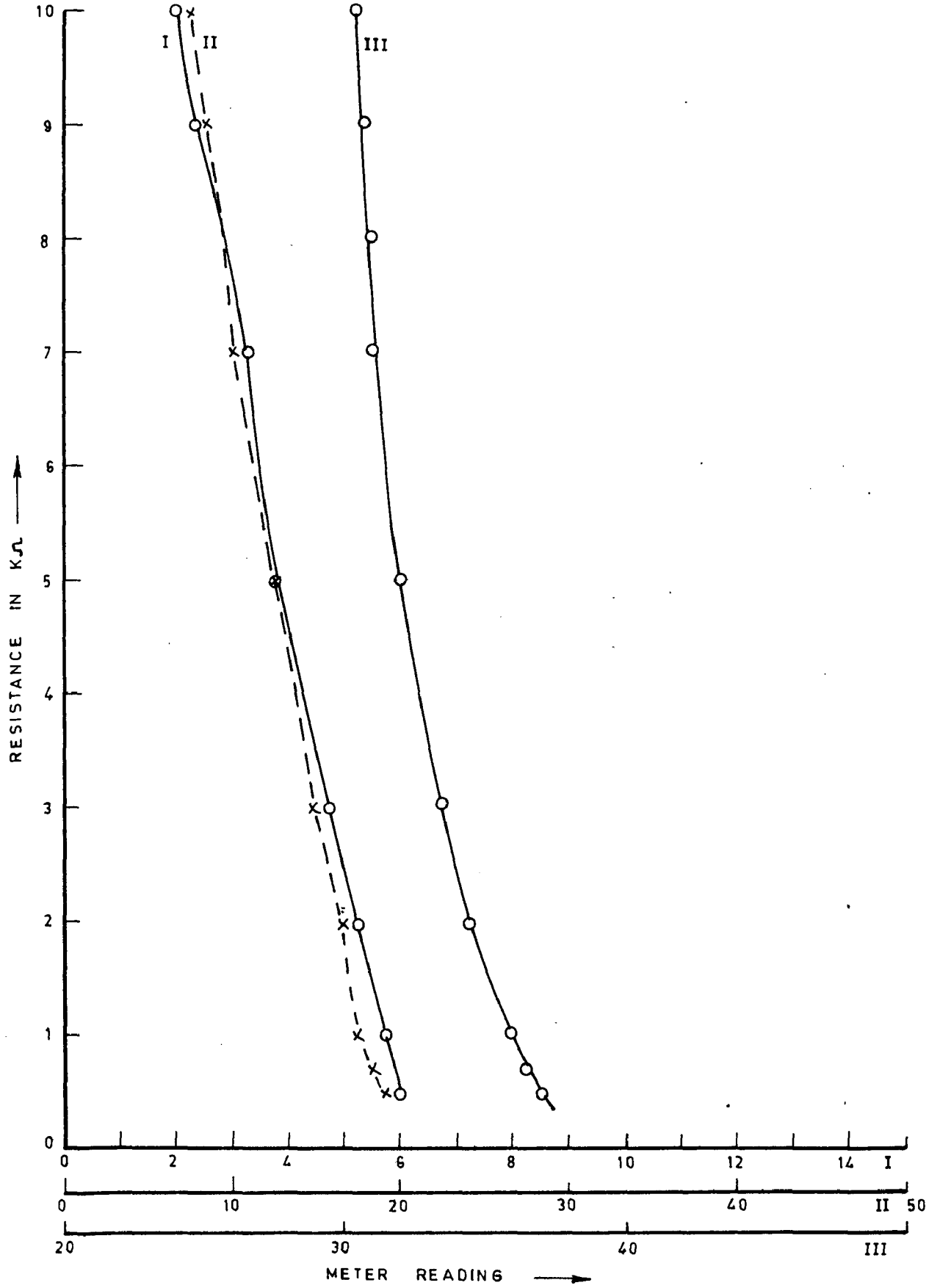

FIG. 15 - BLOCK ROTOR TEST CALIBRATION CURVE FOR STATOR POINTS

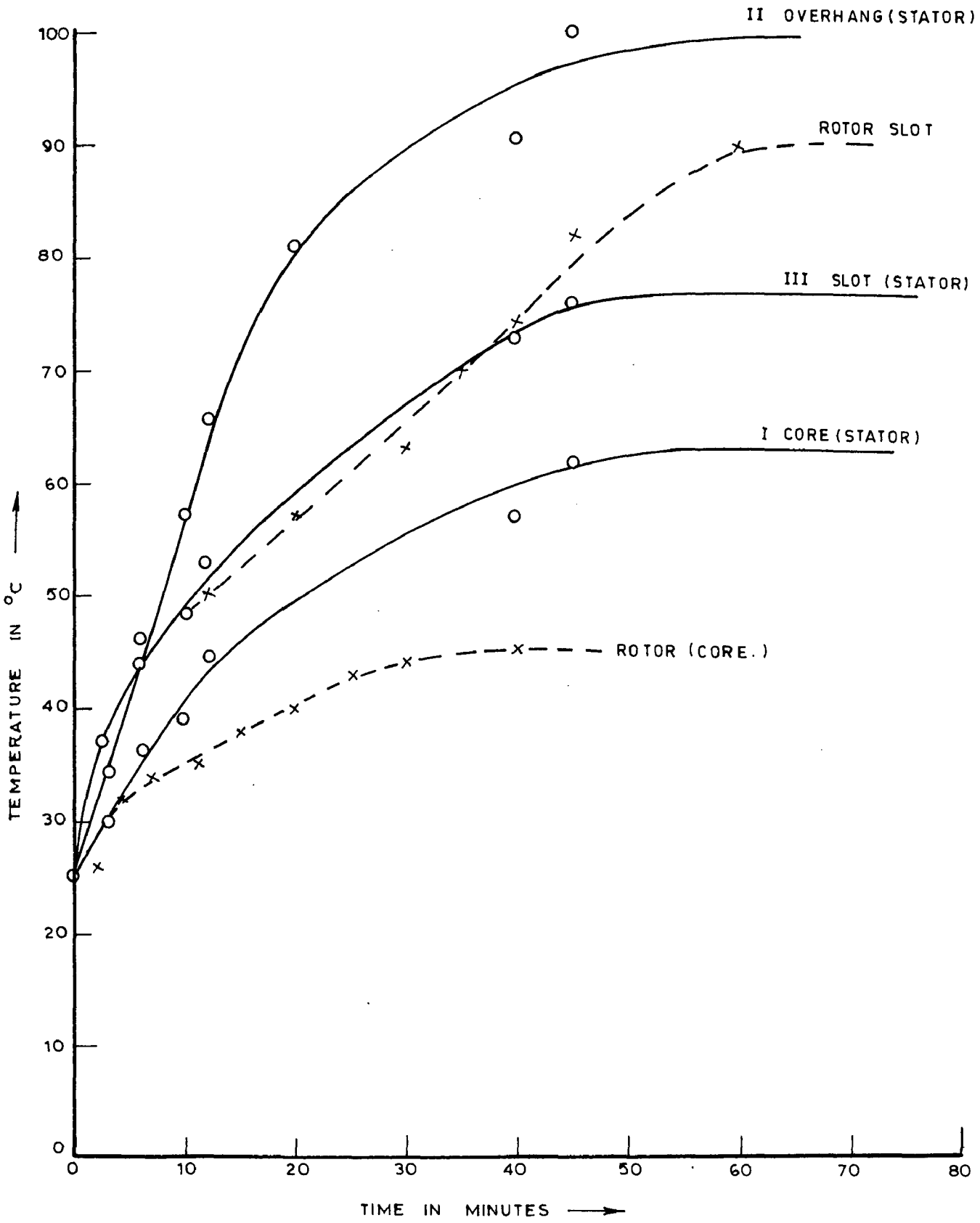

FIG. 16 ∠ BLOCK ROTOR TEST

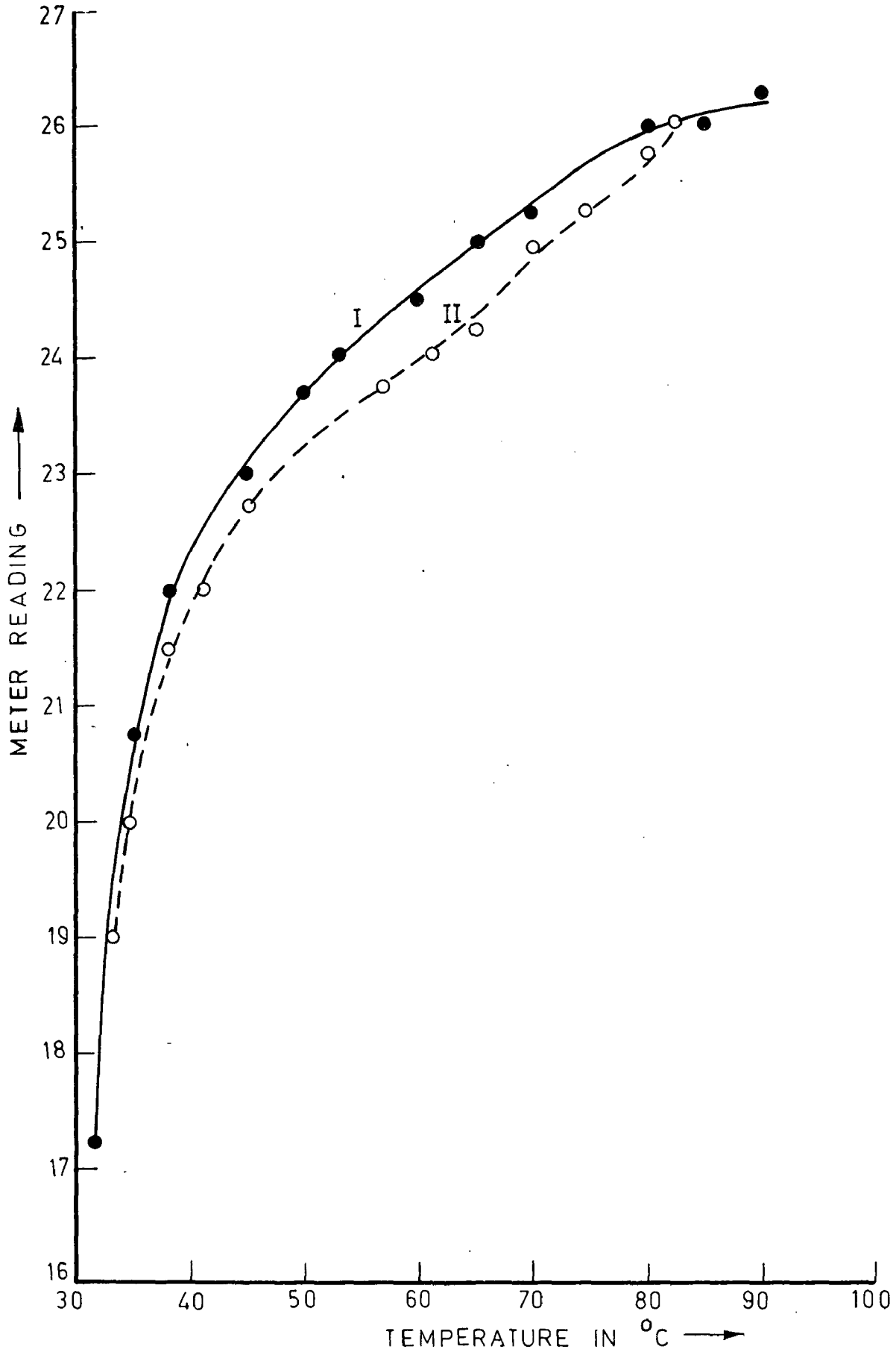

FIG. 17 - CALBRATION CURVE FOR LOAD TEST 5 Amp. LOAD

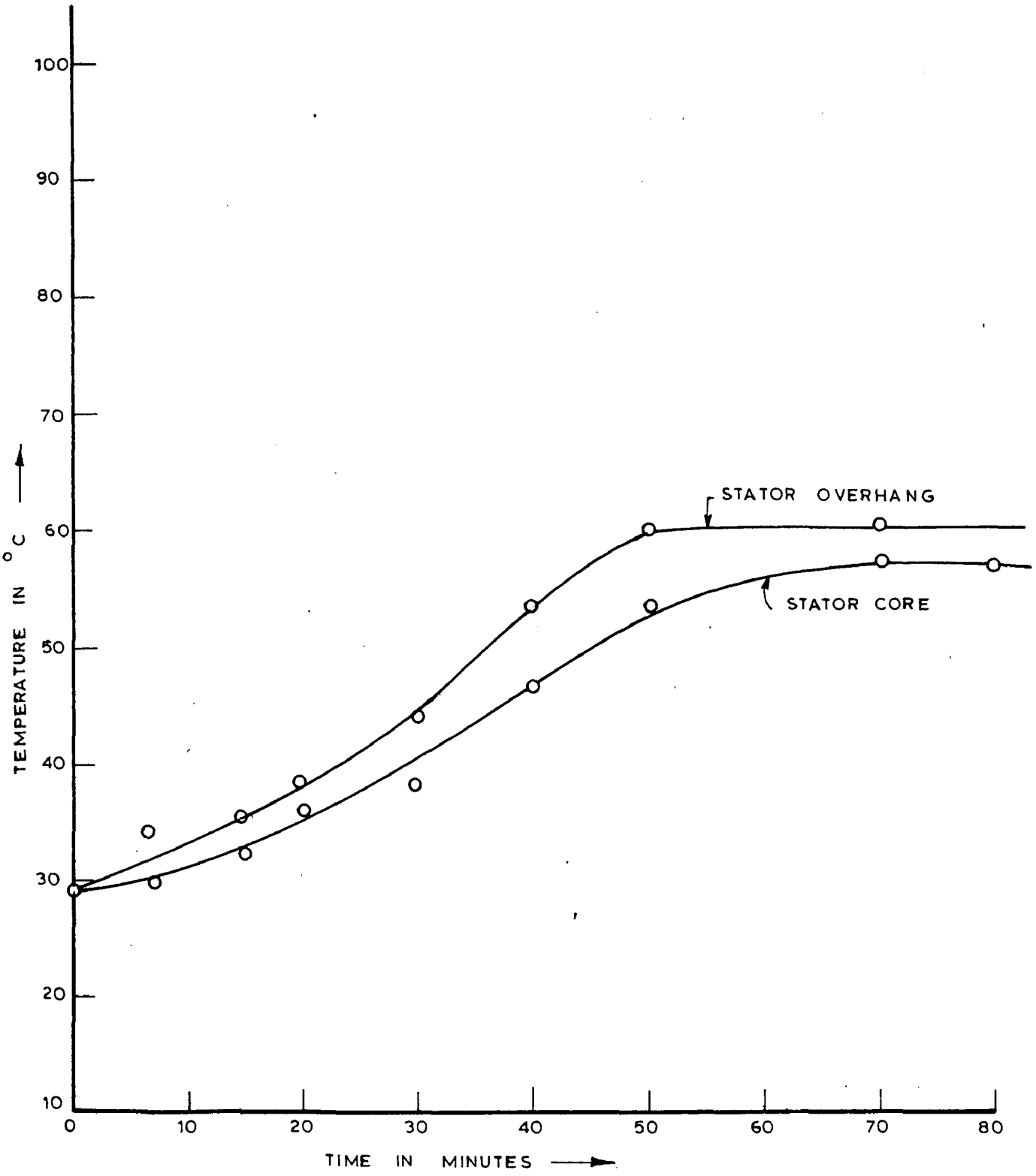

FIG. 18 _ LOAD TEST (5 Amp. load)

CHAPTER V

CONCLUSION

The temperatures at different points in electrical machine have been found out both theoretically and experimentally in this dissertation. The theoretical calculations have been made by using equivalent thermal circuit approach. The errors in the results are due to some approximations and also due to approximate available data for the machine. The results can be improved by taking the exact data of machine and also by reducing the assumptions. The temperatures at the hot spots (three in stator and two in rotor) are measured by using an instrumentation scheme with thermistors as sensing elements. The stator points temperature were measured directly. The rotor points temperature were measured by using a telemetry scheme. The signals from both the rotor points were mixed and then transferred to measuring instrument by using a telemetry unit. The signals were separated out by filters and then rectified to give direct meter reading. The problem was faced in mixing and separation of signals. Some superfluous signals were also observed. These superfluous signals were eliminated to a great extent by using filters. This scheme can be improved upon by using a better mixer and filter units.

APPENDIX-I

Values of Thermal Conductivities

Material	λ W/°C cm	Material	λ W/°C/cm
Copper	380x10^{-2}	Slot insulation of armature winding of d.c. machine and rotor of asynchronous machine	
Aluminium	220x10^{-2}		
Silver	420x10^{-2}		
Steel laminations along the layers			
Each Silicon content	(48 to 35)x10^{-2}		
Medium silicon content	(30 to 26)x10^{-2}	Class A and B	0.10x10^{-2}
Strong silicon content	(20 to 19)x10^{-2}	Class B, F and H	0.16x10^{-2}
Steel laminations ⊥ to the laminations			
With paper insulation	(1.2 to 0.87)x10^{-2}		
With varnish	(4.4 to 3.1)x10^{-2}		
With varnished cloth	(0.15 x 10^{-2}	Same for stator winding of asynchronous and synchronous machines	
With leatheroid	0.25 x 10^{-2}		
Press Board			
Dry	0.180x10^{-2}	class A, B and B	0.1x10^{-2}
Impregnated in oil	0.250x10^{-2}		
Micanite	0.20 x10^{-2}		
Asbestos	0.19x10^{-2}		
C porcelain	(1.5 to 1.69)x10^{-2}	class B (compounded)	
Glass	1.1 x 10^{-2}	F and H	0.16 x 10^{-2}
Wood	0.11x10^{-2}		
Laminated insulation	(0.226 to 0.276)x10^{-2}		
Air with 760 cm of mercury at 40°c	0.0266x10^{-2}		
H_2 with 40°c	0.190x10^{-2}		
Water (40°c)	0.633x10^{-2}		
Transformer oil (40°c)	0.164x10^{-2}		

APPENDIX-II

Values of coefficient c_o for Heated Surfaces in Stationary Air

Characteristic of surface	c_o w/°c cm^2
Iron or Steel surface filled and covered with varnish (and coron and surface).	1.42×10^{-3}
Steel or Iron surface not filled but covered with varnish	1.67×10^{-3}
Enamelled copper surface	1.33×10^{-3}

With a motion of air to the surface of the wall, the coefficient of heat transfer is significantly increased and given by

$$c = 10^{-3}[1 + 0.54v^2] \text{ watts/°c.cm}^2 \quad \ldots (1)$$

Formula (1) can be used for calculating the heat transfer of the overhang portion of the stator winding.

APPENDIX XII

Temperature calculations for 150 H.P., 3300 Volts, 3-Phase, 50 HZ, 6 Pole synchronous r.p.m. slip-ring induction motor. Full load efficiency = 0.91, P.F. = 0.86, complete design of the machine is given in reference [14].

Thermal Calculations for Stator Part

$$R_i = \frac{\delta_i}{\lambda_i S_i} \frac{cm}{Watt/^oc\ cm.cm^2} = {}^oc/w$$

δ_i = Thickness of slot insulation = 0.15 cm (micanite)

λ_i = Thermal conductivity of insulation (Appendix 1) = 0.2×10^{-2} w/^{o}c.c

$S_i = S_D \times$ Perimeter of slot $[(n_b + 1)l']$

S_D = Number of stator slots = 90

n_b = Number of ventilating ducts = 2

l' = Axial length of stator core = $\frac{25-2}{3}$ = 7.66 cm
packet

Perimeter of slot = $2[W_{oo} + d_{oo} - hw]$

width of slot W_{oo} = 0.9 cm

Depth of slot d_{oo} = 5.2 cm

Wedge = 0.3 cm

Perimeter of slot = 2[0.9 + 5.2 - 0.3] cm

= 11.6 cm

$S_i = 90 \times 11.6 \times (2+1)7.66\ cm^2 = 23991.12\ cm^2$

$$R_i = \frac{0.15}{0.2 \times 10^{-2} \times 23991.12} = 0.0031261^oC/W$$

Thermal resistance of overhang portion

$$R_{overhang} = \frac{\delta_i}{\lambda_i S_{overhang}} + \frac{1}{\alpha_{overhang} \cdot S_{overhang}}$$

δ_i = Thickness of insulation of coil = 0.025 cm

λ_i = Thermal conductivity of coil insulation (Appendix 1)

= 0.15×10^{-2} W/°C cm.

$S_{overhang}$ = Surface area of the overhang portion

= S_0 × Perimeter of coil × length of overhang

Perimeter of coil = 2[4.35 + 0.6] = 9.9 cm

Pole pitch $\tau = \frac{\pi D_{in}}{No.\ of\ poles} = \frac{\pi \times 65}{10} = 20.41$ cm

Length of overhang for one turn = 2.5τ + 24 cm = 2.5×20.41+24

= 70.94 cm

Length of overhang for one conductor = 35.47 cm

$S_{overhang}$ = 90×9.9×35.47 cm^2 = 31609.77 cm^2

$c_{overhang}$ coo (Appendix II) = 1.33×10^{-3} W/°c cm^2

$$R_{overhang} = \frac{0.025}{0.15 \times 10^{-2} \times 31609.77} + \frac{1}{1.33 \times 10^{-3} \times 31609.77}$$

$R_{overhang}$ = 0.0003279 + 0.0214117 = 0.021939°C/W

$$R_{winding} = \frac{\text{Length of conductor}}{12 \times S_c \times \text{Number of conductors in slot} \times \text{cross sectional area of one conductor} \times \text{thermal conductivity of copper}}$$

$$= \frac{25}{12 \times 90 \times 24 \times 0.5 \times 0.125 \times 3.8}$$

$R_{winding} = \frac{25}{6156} = 0.004061078$ °C/W

Thermal resistance from coil to the cooling air in radial ventilating ducts =

$$R_{v.d.} = \frac{\delta_i}{\lambda_i \cdot S_{v.d}} + \frac{1}{a_{v.d.} \times S_{v.d.}}$$

δ_i = Slot insulation thickness = 0.15 cm

$_i$ = Thermal conductivity of slot insulation (mica)(Appendix 1)

= 0.2×10^{-2} W/°C cm

$\frac{l_i}{\delta} = \frac{25}{20.41} = 1.225$

Peripheral velocity = $\pi D_0 n$ = $\pi \times 0.65 \times 10$ = 20.41 m/sec.

See Fig.8(a) Mean velocity in v.d. = $0.4 \times v_{peripheral}$

= 0.4×20.41 m/sec

= 0.164 m/sec

See Fig.8(b) $a_{v.d.} = 40\times10^{-4}$ W/°C cm^2

$S_{v.d.}$ = S_0 x Perimeter of coil x width of radial v.d.s x n_b

= $90 \times 2[4.9+0.9] \times 1 \times 2$ = 2030 cm^2

$$R_{v.d.} = \frac{0.25}{0.2\times10^{-2}\times2030} + \frac{1}{40\times10^{-4}\times2030}$$

$R_{v.d.}$ = 0.0379195 + 0.1197318 = 0.1556513 °C/W

$$R_{cg} = \frac{1}{a_g U_g} + \frac{\ell'}{\delta \times q U_g}$$

a_g = H.T. coefficient in the radial ventilating ducts

from Fig. 8 = 40×10^{-4} W/cm^2 C°

U_g = Lateral heat dissipating surface of all pockets

S_g = $\pi(D_o - d_{co})\, d_{co}(n_b+1)$ = $\pi(64.6 - 4.6)4.6(2+1)$ = 3466.56 cm^2

D_o = Outside diameter of stator can. = 64.6 cm

d_{co} = Depth of stator core can = 4.6 cm

ℓ' = Length of stator packet = $\frac{\text{Gross length of core}}{5}$

= $\frac{22}{5}$ cm = 7.66 cm

$_q$ = Thermal conductivity of core material ⊥ lar to laminations

(Appendix 1) = 4×10^{-2} W/°C cm

$$R_{cq} = \frac{1}{40\times10^{-4}\times3466.56} + \frac{7.66}{6.4\times10^{-2}\times3466.56}$$

$$R_{cq} = 0.0721176 + 0.009207 = 0.0813246\ ^{o}c/v$$

$$R_{cp} = \frac{1}{\frac{1}{R_{ont}} + \frac{1}{R_{int}}} = \frac{1}{a_{ont}\cdot S_{ont} + a_{int}\cdot S_{int}}$$

a_{ont} = Heat transfer coefficient of the external surface of stator core packet = $0.0018\ v/^{o}c\ cm^{2}$

S_{ont} = External surface of the stator packet

$= \pi D_{o}\, l'(n_{D}+1)\ cm^{2}$

$= \pi 34.66 \times 7.66(2+1) = 6103.8283\ cm^{2}$

a_{int} = Heat transfer coefficient of the internal surface of the core packet with large air gap from Fig.8 = $40\times10^{-4}\ v/^{o}c\ cm^{2}$

S_{int} = Internal surface of the stator packet

$= \pi D_{i}\, l'(n_{D}+1)\ cm^{2}$

$= \pi 65\times7.66(2+1) = 4690.218\ cm^{2}$

$$R_{cp} = \frac{1}{(0.0018\times6103.8283) + (40\times10^{-4}\times4690.218)}$$

$$= \frac{1}{10.989509 + 10.760372} = \frac{1}{29.756762}$$

$$R_{cp} = 0.0336058\ ^{oc}/v$$

$$R_{c} = \frac{1}{\frac{1}{R_{cq}} + \frac{1}{R_{cp}}} = \frac{1}{\frac{1}{0.0813246} + \frac{1}{0.0336058}}$$

$$R_{c} = \frac{1}{12.296602 + 29.756762} = \frac{1}{71.809990} = 0.0139256\ ^{o}c/v$$

$$\theta_{slot} = R_{winding} \cdot R_{v.d} \cdot R_l \left[P_{overhang} \left(1 + \frac{R_l}{R_{core}}\right) + P_{core} \left(1 + \frac{R_{winding}}{R_{overhang}}\right) + P_{slot} \left(1 + \frac{R_{winding}}{R_{overhang}}\right)\left(1 + \frac{R_l}{R_{core}}\right)\right]$$

$$\theta_{slot} = \frac{}{(R_{v.d} \cdot R_l + R_{v.d} R_{winding} + R_{winding} R_l)\left(1 + \frac{R_l}{R_{core}}\right) - R_{v.d} \cdot R_l \left(1 + \frac{R_l}{R_{core}}\right) - R_{winding} \cdot R_{vd} \cdot \left(1 + \frac{R_{winding}}{R_{overhang}}\right)}$$

$R_{winding} = 0.0006\,1078\ ^{o}c/w$

$R_{v.d} = 0.1556515\ ^{o}c/w$ $\qquad P_{core} = 3740$ watts

$R_l = 0.0032061\ ^{o}c/w$ $\qquad$ copper loss $= 2740$ watts

$R_{overhang} = 0.021139\ ^{o}c/w$

$R_{core} = 0.0159256\ ^{o}c/w$

$$\theta_{slot} = \frac{0.00[illegible][1556 (1.224450) + 3740(1.1851041) + 1102(1.4511451)}{(0.0[illegible]065 + 0.0006519 + 0.0000126)(1.4511451) - 0.[illegible]065 (1.224450) - 0.0006519(1.1851041)}$$

$$= \frac{0.00[illegible][1956.7203 + 4433.2009 + 1657.2054]}{0.0020[illegible]2 - 0.0005957 - 0.0007688}$$

$$= \frac{0.0[illegible]}{0.0[illegible]} = 53.95\ ^{o}c$$

$$\theta_{overhang} = \frac{P_{overhang} R_{winding} + \theta_{slot}}{1 + \frac{R_{winding}}{R_{overhang}}}$$

$$= \frac{1701[illegible]0.0006\,1078 + 53.9576}{1.1851041} = 50.87\ ^{o}c$$

$$\theta_c = \frac{P_{core} \times R_g + \theta_{coil}}{1 + \frac{R_g}{R_{core}}}$$

$$= \frac{2740 \times 0.0031201 + 53.35}{1.2240459} = 53.12^{\circ}c$$

$$\theta_{coil} = \frac{\left[P_{coil}\left(2 + \frac{R_g}{R_{core}}\right) + P_{core}\right] R_{core}}{1 + \frac{R_g}{R_{coil}} + \frac{R_{core}}{R_{coil}}}$$

$$R_{coil} = \frac{R_{overhang} \times R_{v.d}}{R_{overhang} + R_{v.d}} = \frac{0.021959 \times 0.1556513}{0.021959 + 0.1556513} = \frac{0.0034189}{0.17755905}$$

$$= 0.0192519\ ^{\circ}c/w$$

$$\theta_{coil} = \frac{[2740(1.2240459) + 2740]\ 0.0192519}{1 + \frac{0.0031201}{0.0192519} + \frac{0.0192519}{0.0192519}}$$

$$= \frac{(3355.0 + 2740)\ 0.0192519}{1 + 0.1620476 + 1.0000000}$$

$$= \frac{52.8823}{1.6620476} = 52.97\ ^{\circ}c$$

$$\theta_c = \frac{P_{core} R_g + \theta_{coil}}{1 + \frac{R_g}{R_{core}}} = \frac{2740 \times 0.0031201 + 52.92}{1.2240459}$$

$$= 52.51\ ^{\circ}c$$

Thermal Calculations for Rotor Bars:

$$R_g = \frac{\delta_g}{1} \frac{m}{\delta_g\ w/^{\circ}c.cm} = {}^{\circ}c/w$$

δ_g = Thickness of slot insulation = 0.05 cm

λ_i = Thermal conductivity of insulation (Appendix 1) = 0.2×10^{-2} w/°c

D_i = D_r x Perimeter of slot $[(n_b \cdot 1)\ l']$

D_r = Number of rotor slots = 120

n_b = Number of ventilating ducts = 2

l' = Axial length of rotor core packet = $\frac{25 - 2}{3}$ = 7.66 cm

Perimeter of slot = $2[w_{rs} + d_{rs} + h_w]$

Width of rotor slot = w_{rs} = 0.5 cm

Depth of rotor slot = d_{rs} = 3.7 cm

Height of wedge = h_w = 0.3 cm

Perimeter of slot = 2[0.5+3.7 + 0.3] = 7.8 cm

D_i = 120 x 7.8 (2 + 1) 7.66 = 21505.20 cm^2

Π_i = $\frac{0.05}{0.2 \times 10^{-2} \times 21505.20}$ = 0.0006979 °c/w

Thermal resistance of overhang portion

$$\Pi_{overhang} = \frac{\delta_i}{\lambda_i A_{overhang}} + \frac{\lambda}{a_{overhang} \times A_{overhang}}$$

δ_i = Thickness of insulation of coil = 0.1 cm

λ_i = Thermal conductivity of coil insulation (Appendix 1)
= 0.15×10^{-2} w/°c cm

$A_{overhang}$ = Surface area of the overhang portion
= 2π D_r x Perimeter of coil x length of overhang

Perimeter of coil = 2[1.4 + 0.4] = 3.6 cm

Length of the overhang for one conductor = 35.47 cm
(as calculated for stator portion)

$A_{overhang}$ = 2x120 x 3.6 x 35.47 = 30646.0 cm^2

With motion of air 1 to the surface of the coil, the coefficient of heat transfer

$$\alpha_{overhang} = 10^{-3}[1 + 0.542v^2]$$

v = Peripheral speed of air in m/sec

$= \pi D n_b = \pi \times 0.648 \times 10 = 20.3472$ m/sec.

Velocity of air at end surface = 0.1×20.3472

$$\alpha_{overhang} = 10^{-3}[1 + 0.54 \times (2.03472)^2]$$

$$= 3.2356461 \text{ w/}^{o}\text{c m}^2$$

$$R_{overhang} = \frac{0.1}{0.15\times10^{-2}\times30646.03} + \frac{1}{3.2356461\times30646.03}$$

$R_{overhang} = 0.0221703 + 0.0100347 = 0.0322 \ ^{o}c/w$

$$R_{winding} = \frac{\text{length of conductor}}{12 \times \text{No. of conductors in slot} \times \text{cross sectional area of one conductor} \times \text{thermal conductivity of copper}}$$

$$R_{winding} = \frac{25}{12\times210\times2\times1.9\times0.9\times3} = 0.0053572 \ ^{o}c/w$$

Thermal resistance from coil to the cooling air in radial ventilating ducts =

$$R_{v.d.} = \frac{\delta_i}{\lambda_i \times S_{v.d.}} + \frac{1}{\alpha_{v.d.} \times S_{v.d.}}$$

δ_i = Slot insulation thickness = 0.05 cm

λ_i = Thermal conductivity of slot insulation (micanite) (Appendix I) = 0.2×10^{-2} w/^{o}c cm

$\alpha_{v.d.}$ Heat transfer coefficient in v.d. = 40×10^{-4} w/^{o}c cm^2 as calculated for stator part.

$S_{v.d.}$ = S_p = Perimeter of coil x width of radial v.d. x n_b

= $120 \times 2[3.7 + 0.5] \times 1 \times 2 = 2016$ cm^2

$$R_{v.d.} = \frac{0.03}{0.2 \times 10^{-3} \times 2016} + \frac{1}{40\times10^{-4}\times2016}$$

$$R_{v.d.} = 0.0074405 + 0.1240079 = 0.1314403\ ^{o}c/v$$

$$R_{c.e} = \frac{1}{a_q S_q} + \frac{l'}{a_q S_q}$$

a_q = Heat transfer coefficient in the radial ventilating ducts from Fig.8 = 40×10^{-4} v/°c cm^2

S_q = Lateral heat dissipating surface of all packets

= $(D_i + d_{cr})\, d_{cr}\, (n_p + 1)$ = $\pi(40.2+4.6)4.6(24+1)$

= 2207.9296 cm^2

D_i = Internal diameter of rotor = 40.2 cm

d_{cr} = Depth of rotor core = 4.6 cm

l' = Length of rotor packet = $\frac{\text{Gross length of core}}{9}$

= $\frac{22}{3}$ = 7.66 cm

q = Thermal conductivity of core material i to laminations (Appendix 1) = 6×10^{-2} v/°c cm

$$R_{cq} = \frac{1}{40\times10^{-4}\times2207.9296} + \frac{7.66}{6\times4\times10^{-2} \times 2207.9296}$$

$$R_{cq} = 0.109269 + 0.01595 = 0.125219\ ^{o}c/v$$

$$R_{cp} = \frac{1}{\frac{1}{R_{ont}} + \frac{1}{R_{int}}} = \frac{1}{a_{ont.} S_{ont.} + a_{int} S_{int.}}$$

a_{ont} = Heat transfer coefficient of the external surface of rotor core packet = 0.0018 v/°c cm^2

S_{ext} = External surface of the rotor pocket

= $\pi D_0 l' (n_0 + 1)$

= $\pi \times 64.0 \times 7.66 (2+1) = 4675.7065$ cm^2

C_{int} = Heat transfer coefficient of the internal for surface of the core pocket with large air gap

$C = 3.6\ d^{-3.2}\ v^{0.8} \times 10^{-4}$ where, d = diameter of duct. v = peripheral velocity of air in m/sec.

$C = 3.6(0.01)^{-3.2}(20.4)^{0.8} \times 10^{-4}$ w/^{0}c cm^2

$= 3.6 \times 11.18 \times 10^{-4} \times 2.5119 = 100.55690 \times 10^{-4}$ w/^{0}c cm^2

S_{int} = Internal surface of the rotor pocket

$= \pi D_1 l' (n_0 + 1)$

$= \pi \times 40.2 \times 7.66 (2+1) = 3477.9760$

$$R_{op} = \frac{1}{(0.0010 \times 4675.7065) + (100.55690 \times 3477.9760) \times 10^{-4}}$$

$$R_{op} = \frac{1}{8.4166197 + 34.979275} = \frac{1}{43.395869} = 0.0230469\ ^0c/w$$

$$R_c = \frac{1}{\frac{1}{R_{cg}} + \frac{1}{R_{op}}} = \frac{1}{\frac{1}{0.129219} + \frac{1}{0.0230469}}$$

$$R_{core} = \frac{1}{8.1156919 + 43.395869} = \frac{1}{51.505434} = 0.0194154\ ^0c/w$$

$R_{winding} = 0.0353572\ ^0c/w$ $\quad P_{core} = 0$

$R_{w.c.} = 0.1524433\ ^0c/w$ $\quad$ Copper loss = 2860 watts

$R_i = 0.0003979\ ^0c/w$ $\quad P_{overhang} = 1660.3952$

$R_{overhang} = 0.01220\ ^0c/w$ $\quad P_{slot} = 119.6060$

$D_{core} = 0.0210210$ %/w

$\theta_{clad\ portion\ of\ wdg.} = \dfrac{D_{standing}\,D_{v.c.}\,D_{\ell}\left[D_{overhang}\left(1+\frac{D_{\ell}}{D_{core}}\right)+D_{core}\left(1+\frac{D_{standing}}{D_{overhang}}\right)+D_{clad}\left(1+\frac{D_{standing}}{D_{overhang}}\right)\left(1+\frac{D_{\ell}}{D_{core}}\right)\right]}{\left(D_{v.c.}D_{\ell}+D_{v.c.}D_{standing}+D_{standing}D_{\ell}\right)\left(1+\frac{D_{standing}}{D_{overhang}}\right)\left(1+\frac{D_{\ell}}{D_{core}}\right)-D_{v.c.}D_{\ell}\left(1+\frac{D_{\ell}}{D_{core}}\right)-D_{standing}D_{v.c.}\left(1+\frac{D_{standing}}{D_{overhang}}\right)}$

$= \dfrac{0.00[illegible]}{0.0[illegible]1.55[illegible]16 - 0.0[illegible]1.05[illegible]47 - 0.0[illegible]}$

1.47774

$= \dfrac{0.0[illegible]}{0.0[illegible]}$

$= \dfrac{0.0[illegible]}{0.0[illegible]} = 19.222[illegible]$ %

$\theta_{overhang} = \dfrac{D_{core} \times D_{standing} + \theta_{clad}}{1+\frac{D_{standing}}{D_{overhang}}}$

$= \dfrac{[illegible] \times 0.[illegible] + 19.[illegible]}{1+0.47774}$

$= 19.[illegible]$ %

$\theta_{core} = \dfrac{D_{core} \times D_{\ell} + \theta_{clad}}{1+\frac{D_{\ell}}{D_{core}}} = \dfrac{19.[illegible]}{1.0[illegible]} = 10.[illegible]$ %.

$\theta_{coil} = \dfrac{\left[D_{coil}\left(2+\frac{D_{\ell}}{D_{core}}\right)+D_{core}\right]D_{core}}{1+\frac{D_{\ell}}{D_{coil}}+\frac{D_{core}}{D_{coil}}}$

$$R_{coil} = \frac{R_{overhang} \times R_{v.d.}}{R_{overhang} + R_{v.d.}} = \frac{0.01226 \times 0.1314483}{0.01226 + 0.1314483}$$

$$= \frac{0.0016115}{0.1437085} = 0.0112136$$

$$\theta_{coil} = \frac{[2860 \times 1.0359147 + 01.0.0198154}{1 + 0.0621834 + 1.7314154}$$

$$= \frac{57.522316}{2.7955988} = 20.59\ ^{o}_{o}$$

$$\theta_{core} = \frac{P_{core} \frac{R_1}{} + \theta_{coil}}{1 + \frac{R_1}{R_{core}}}$$

$$= \frac{20.590757}{1.0359147} = 19.87\ ^{o}_{o}$$

APPENDIX IV

Block Rotor Test

Voltage	Current	Watts W_1	Watts W_2	Watts $(W_1 + W_2)$
130 V	7.5 A	97x4	-32x4	660
107 V	6 A	123x4	-20x4	412
74 V	4 A	55x4	-10x4	180
53 V	3 A	30x4	-5x4	100

Light Running Test

Voltage	Current	W_1 Watts	W_2 watts	$W_1 + W_2$ watts
100 V	3.5 A	10x16	5x16	240
150 V	2.2 A	10x16	2x16	192
200 V	1.2 A	12x16	2x16	224
250 V	2.2 A	15x16	0	240
300 V	1.5 A	20x16	-2x16	288
350 V	2A	30x16	-10x16	320
400 V	2.0 A	42x16	-20x16	352

Resistance Measurement of Stator

Current (Ampere)	Voltage (volts)	Resistance
2.4	8.8	3.66
3.8	14	3.68
5.6	20	3.57

Calculation of losses

Friction and windage loss = 140 watts

No load I^2 R loss = $3\ I^2 R = 5.18$ watts

Core loss = 290 - 140 - 5.18 = 84.82 watts

Stator I^2 R loss = $3\ (7.5)^2 \times \frac{2.6}{2} = 300$ watts

Output = 5x746 = 3730 watts.

APPENDIX-V

Thermal Calculations for Stator Parts

$$R_i = \frac{\delta_i}{\lambda_i A_i}$$

δ_i = Thickness of slot insulation = 0.05 cm

λ_i = Thermal conductivity of insulation (Appendix 1)

= 0.2×10^{-2} W/°C cm

A_i = Area of insulation

= S_0 × Perimeter of slot $[(n_b + 1)\ell']$

S_0 = Number of stator slots = 36

n_b = Number of ventilating ducts = 0

ℓ' = Axial length of stator core packet = L = 10.0 cm

Perimeter of slot = $2[W_{SO} + d_{OS} + h_w]$

Width of stator slot W_{SO} = 1.2 cm

Depth of stator slot d_{OO} = 2.2 cm

Wedge = 0.3 cm

Perimeter of slot = 2[1.2+2.2 + 0.3] = 6.2 cm

A_i = 36×6.2×10.0 = 2410.56 cm^2

$$R_i = \frac{0.05}{0.2 \times 10^{-2} \times 2410.56} = 0.010371\ ^\circ C/watts$$

Thermal resistance of overhang portion

$$R_{overhang} = \frac{\delta_i}{\lambda_i L_{overhang}} + \frac{1}{a_{overhang} \times B_{overhang}}$$

δ_i = Thickness of insulation of coil = 0.02 cm

λ_i = Thermal Conductivity of coil insulation (Appendix 1)

= 0.15×10^{-2} W/°C

$S_{overhang}$ = Surface area of the overhang portion

= S_0 x Perimeter of coil x length of overhang

Perimeter of coil = 2[1.75 + 1.10] = 5.7 cm

Length of overhang = 2.3x11.57 + 24 = 50.63 cm = 11.57 for one turn

Length of overhang = $\frac{50.63 \text{ cm}}{2}$ = 25.315 cm for one conductor

S_{OH} = 36x5.7x25.315 = 5194.638 cm^2

σ_{OH} = 1.33×10^{-3} $\mho/^{o}c$ cm^2 (See Appendix II)

$$R_{OH} = \frac{0.02}{0.15 \times 10^{-2} \times 5194.638} + \frac{1}{1.33 \times 10^{-3} \times 5194.638}$$

R_{OH} = 0.0025667 + 0.1447417 = 0.1473084 $^{o}c/\mho$

$$R_{winding} = \frac{\text{Length of conductor}}{12 \times S_0 \times \text{Number of conductors in slot} \times \text{cross sectional area of one conductor} \times \text{thermal conductivity of copper}}$$

$R_{winding} = \frac{10.0}{12 \times 56.33 \times \frac{1}{4} \times (101)^2 \times 3.0}$ = 0.02496 $^{o}c/\mho$

Number of conductors in a slot

Pole pitch $\tau = \frac{\pi D}{P} = \frac{\pi \times 14.75}{4}$ = 11.57

Flux per pole $\phi_p = D_{av} \times \tau \times L$

= 0.44x0.1157x0.103 = 5.498×10^{-3} mwb.

Stator turns per phase $T_s = \frac{E_p}{4.44 f \times \phi_p \times K_{ws}}$

$= \frac{400/\sqrt{3} = 230.94688}{4.44 \times 50 \times 5.498 \times 10^{-3} \times 0.955}$

= 198.13026

Total stator conductors = 6 T_s = 6x198.13026

Stator conductors/slot = $\frac{6 \times 192.18026}{96}$ = 33

Thermal resistance R_{core} from core to the cooling air

$$R_{core} = \frac{\lambda}{\frac{1}{R_{ext}} + \frac{\lambda}{R_{int}}} = \frac{1}{C_{ext.} S_{ext.} + \alpha_{int} S_{int}}$$

C_{ext} = Heat transfer coefficient of the external surface of the stator core packet = 0.0010 W/°C

S_{ext} = $\pi D_o l' (n_d + 1)$ = $\pi \times 23.2 \times 10.0$ = 786.7504

C_{int} = Heat transfer coefficient of the internal surface of stator core packet from Fig. 8.

$\frac{l}{t}$ = $\frac{10.0}{11.57}$ = 0.8334 from Fig. 8.

Mean velocity = 0.40 x Peripheral velocity

= 0.40 x π x 0.1475 x 25

= 5.5570 m/sec.

C_{int} from Fig. 11.3 = 30×10^{-4} W/°C cm^2

S_{int} = $\pi D_i l' (n_d + 1)$ = $\pi \times 14.75 \times 10.0$ = 500.202

$$R_o = \frac{1}{0.0010 \times 786.7504 + 30 \times 10^{-4} \times 500.202}$$

$$R_o = \frac{1}{1.4161692 + 1.500606} = \frac{1}{2.91677} = 0.3428449$$

R_{coil} = $R_{overhang}$ = 0.1473034

$$\theta_{coil} = \frac{\left[P_{coil}\left(1 + \frac{R_i}{R_{core}}\right) + P_{core}\right] R_{core}}{1 + \frac{R_i}{R_{coil}} + \frac{R_{core}}{R_{coil}}}$$

$$= \frac{[96(1 + \frac{0.210271}{0.9428449}) + 84.02]0.9428449}{1 + \frac{0.210271}{0.1479654} + \frac{0.9428449}{0.1479654}}$$

$$= \frac{[242.2664) + 84.02]\ 0.9428449}{1 + 0.05907 + 2.9279954} = \frac{236.10491}{5.4204654} = 39.79\ ^{o}c.$$

$$\theta_c = \frac{P_{core}\ D_1 + \theta_{coil}}{1 + \frac{D_1}{0.9428449}} = \frac{40.6711}{1.0382295} = 37.37$$

Thermal Calculation for Rotor Part

$D_1 = \frac{\delta_1}{\lambda_1 U_1}$

δ_1 = Thickness of slot insulation = 0.25 cm

λ_1 = Thermal conductivity of insulation Table 1 = 0.2×10^{-2} w/°c cm

U_1 = U_r x Perimeter of slot $[n_b + 1)l']$

U_r = Number of rotor slot = 96

n_b = Number of ventilating ducts = 0

l' = Axial length of rotor core packet = 10.0 cm

Perimeter of slot = $2[w_{r0} + d_{r0} - h_v]$

Width of rotor slot w_{r0} = 1.2 cm

Depth of rotor slot d_{r0} = 1.6 cm

Height of wedge h_v = 0.3 cm

Perimeter of slot = 2[1.2+1.6 - 0.3] = 5 cm

U_1 = 96x5x10.0 = 1944 cm^2

$$D_1 = \frac{0.25}{0.2 \times 10^{-2} \times 1944} = 0.0385302\ ^{o}c/w$$

$$D_{overhang} = \frac{D_1}{1\ \lambda_{overhang}} + \frac{1}{a_{overhang}\ \pi\ U_{overhang}}$$

δ_i = Thickness of insulation of coil = 0.1 cm

λ_i = Thermal conductivity of coil insulation Table 1 = 0.15×10^{-2} W/°

$B_{overhang}$ = Surface area of the overhang

= $2 \times D_{ip}$ Perimeter of coil x length of overhang

Perimeter of coil = 2[1.05 + 1.05] = 4.2

Length of overhang = 50.65 cm

$B_{overhang}$ = $2 \times 36 \times 4.2 \times 5065$ = 15510.517 cm^2

With motion of air 1 to the surface of the wall, the coefficient of heat transfer

$$\alpha_{overhang} = 10^{-3}[1 + 0.54\ v^2]$$

v = Peripheral speed of air in motor/sec.

= $\pi\ D\ n_0$ = $\pi \times .145 \times 24$ = 10.9272

Velocity of air on end surface = 0.1×10.9272 = 1.09272

$$\alpha_{overhang} = 10^{-3}[1 + 0.645] = 1.645 \times 10^{-3}$$

$$R_{overhang} = \frac{0.1}{0.15 \times 10^{-2} \times 15510.517} + \frac{1}{1.645 \times 10^{-3} \times 15510.517}$$

$$R_{overhang} = 0.0004292 + 0.0397049 = 0.0401341$$

Thermal resistance R_{core} from core to the cooling air

$$R_{core} = \frac{1}{\frac{1}{R_{ext}} + \frac{1}{R_{int}}} = \frac{1}{\alpha_{ext} \cdot B_{ext} + \alpha_{int} \cdot B_{int}}$$

α_{ext} = Heat transfer coefficient of the external surface of the stator core packet = 0.0018 W/°C cm^2

B_{ext} = $\pi\ D_0\ l'(n_0 + 2)$ = $\pi \times 14.5 \times 10.$ = 491.724

$a_{int} = 1.645 \times 10^{-3}$ v/°c cm^2

$B_{int} = cal.7 \times 10^{-3} = 261.1224$

$\frac{l}{t} = \frac{10.8}{11.57} = 0934$

Mean velocity = 0.4Circumferencal velocity

= 0.48xπ0.145 x 24

= 5.069 m/sec

$$R_{core} = \frac{1}{a_{ext.} U_{cnd} + a_{int.} U_{int}}$$

$$= \frac{1}{0.0010 \times 451.72 + 30 \times 10^{-4} \times 261.1224}$$

$$= \frac{1}{0.895320 + 0.103567} = \frac{1}{1.668469} = 0.599554$$

$R_{coil} = R_{overhang} = 0.0401341$

$$\theta_{coil} = \frac{[P_{coil}(2 + \frac{D_1}{D_{core}}) + P_{core}]R_{core}}{1 + \frac{D_1}{D_{coil}} + \frac{R_{core}}{R_{coil}}}$$

$$= \frac{960(1 + \frac{0.[illegible]}{[illegible]}) .599554}{1 + \frac{0.[illegible]}{0.[illegible]41} + \frac{0.599554}{0.0401341}}$$

$$= \frac{960 \times 1.[illegible] \times 0.599554}{1 + 0.[illegible] + 14.999704}$$

$$= \frac{229.[illegible]}{16.09921} = 13.595 \ ^{o}c$$

$$\theta_{core} = \frac{P_{core} L_g \cdot \theta_{coil}}{1 + \frac{L_1}{R_{core}}} = \frac{13.595}{1.0642991} = 12.77 \ ^{o}c$$

APPENDIX-VI

Summary of Characteristics of Transducers for Measurement of Temperature

Principle	Range	Accuracy	Linearity	Advantages	Disadvantages
Resistance Thermometer	-263°c to +630°c upper limit can be raised to 1649°c	±0.01% possible but dependent on range and material	For platinum ±0.4% from -186°c to ±160°c ±1.2% from +250°c to 615°c	-	Relatively large physical size measuring current may heat element and cause error
Thermistor	-60°c to +[illegible] but upper limit generally 350°c	± 0.01°c at 100 °c	Dependent on type of thermistor	Small r.m.s. can be used with a.c. or d.c.	-
Transistor	0°c to 60°c	± 0.001°c	Exponential characteristics	Highly sensitive	Less stable than thermistor
Electrolytic	Dependent on freezing and boiling points of electrolyte	± 1°c	Non linear dependent on electrolyte	-	-
Ionisation	4000 K to over 13000 K	± 10%	Non linear	Insensitive to pressure between 1 and 10 at c.	-
Inductive Permeability	Below 10 K	No figures available	Non-linear inverse relationship	-	Coils usually kept in liquid hydrogen.
Thermomagnetic	No figures available	-	-	No direct physical contact needed	Empirical calculation required.

Table contd..../-

Principle	Range	Accuracy	Linearity	Advantages	Disadvantages
Capacitive dielectric constant	-40°c to 200°c	No figures available	± 1%	-	Dielectric has to be carefully chosen, many materials have losses that increase with temperature
Thermoelectric thermocouple	-259°c to +1990°c Diff. ranges with in these limits covered by different combination of materials.	±0.2°c for platinum/ platinum rhodium at 1039°c. top of 21% iron constant on from 260°c to 650°c.	Dependent on thermocouple material	Simple	Reference junction required.
Solid thermometer	100-170°K	±0.1% with special selection ±1% without selection	Dependent on temperature coefficient of resistance of material used for probe	-	-
Acoustic	2°K-1650°K	Dependent on method (±2% 250-2500°K)	Cases square root relationship liquid and solids reciprocal relationship	-	-
Ultrasonic	Upto 1900°c	± 4°c	Non-linear	-	Must be calibrated before use
Pyro-electric	4°K-500°K Both it is possible that the upper range could be extended to 150°K	± 6 °K	Non-linear ± 0%	Highly sensitive (10⁻⁵°c can be used for high freq. changes of temperature.	-

REFERENCES

1. KUDLACIK, H.H., WILLYAMS, 'Local Stator Winding Temperature Measurement For Large Turbine Generator Fields', AIEE Transaction on Power Apparatus and Systems, Vol.81, Feb.1963, pp 687-94.
2. Soderberg, C.R., 'Steady Flow of Heat in Large Turbine-Generators', Transaction of the American IEE, 1931, 50, pp 782-797.
3. Johnson, A.I., 'The Application of Computers to the Solution of Induction Motor Thermal Circuits', Transactions AIEE, Vol75, pt.III, 1956, pp 1543-46.
4. Roemberry, G.H., 'The Transient Stalled Temperature Rise of Cast-Aluminium Squirrel-Cage Rotors For Induction Motors', Jr Ibid, Vol.74, Part III, Oct.1955, pp 819-24.
5. Mecky, H.H, 'The Determination of The Transient Temperature Distribution In A Turbo-Alternation Rotor By Means of An Analogue', Proc. IEE Vol. 109C, 1962, pp 126-137.
6. Mc Adams, W.H., 'Heat Transmission (Mc Graw Hill, 3rd edn, 1954).
7. Arnor, A.F., and Chari, M.V.K., 'Heat Flow in The Stator Core of Large Turbine Generators By The Method of Three-Dimensional Finite Element Part I - Analysis By Scalar Potential Formation', IEEE PAS, 1976, pp 1648-56.
8. Arnor, A.F. and Chari, M.V.K., 'Heat Flow in the Stator Core of Large Turbine Generators', By The Method of Three - Dimensional Finite Elements, IEEE PAS, 1976, pp 1657-63.

9. Mac Martin, H.P. and Tarnoiv, O.H., 'The Measurement of The Temperature Rise of The Rotor of A 500 M.W. Generator',, IEEE Trans. PAS, Vol.95, No.2, March/April 1976, pp 630-33.

10. Gupta O.C. and Deval, 'A Novel Technique for the Measurement of Average Rotor Temperature of Brushless Synchronous Machine', IEEE Trans. PAS, 1977.

vol. ? no. pp ?

11. Crump, M.G. and Grady, M.F., 'Direct Measurement of Generating Winding Temperature Using Miniature Transmitter', IEEE, Trans. on PAS, Vol.84, 1965, No.11, pp 1973-79.

12. Mukherji, H.N. and Willyoung, D.M., 'Local Rotor Winding Temperature Measurement For Large Turbine - Generator Fields', IEEE Trans. on PAS, Vol.81, pp 687-694, Feb. 1963.

13. Design of Electrical Machines by Vinogradov.(in Russian).

14. GAINEY, A.K., 'A Course in Electrical Machine Design', (2nd edition 1972).

15. Crocadero D.W., 'Handbook of Telemetry and Remote Control', McGraw-Hill Book.

16. Hyde - Thermistors.

17. Robert E. Obenhaus, 'Sensor Retrofitting of Motors for Protection Against Overtemperature', IEEE Industry Applications Jan./Feb. 1975, pp 24-33.

18. Bottman D.R., Elgan F.L., Woodall R.J., 'Thermal Tracking - A National Approach to Motor Protection', IEEE PAS-93, No.5, Sept/Oct. 1974, pp 1335-1343.

19. Noble J1, 'Thermistor an Industrial Electric Motor Protection', N.Z. Engineering 15 March 1968.

20. Coughlin. R.F. and Driscoll F.F.,'Operational Amplifiers and Linear Integrated Circuits'.

21. Norton,'Handbook of Transducers for Electronics Measuring Cystem'.

22. Graeme J.G.,'Designing With Operational Amplifiers. Burr - Brown series.

23. Mansfield, PH,'Electrical Transaction for Industrial Measurement'.